

BSc Thesis Applied Mathematics

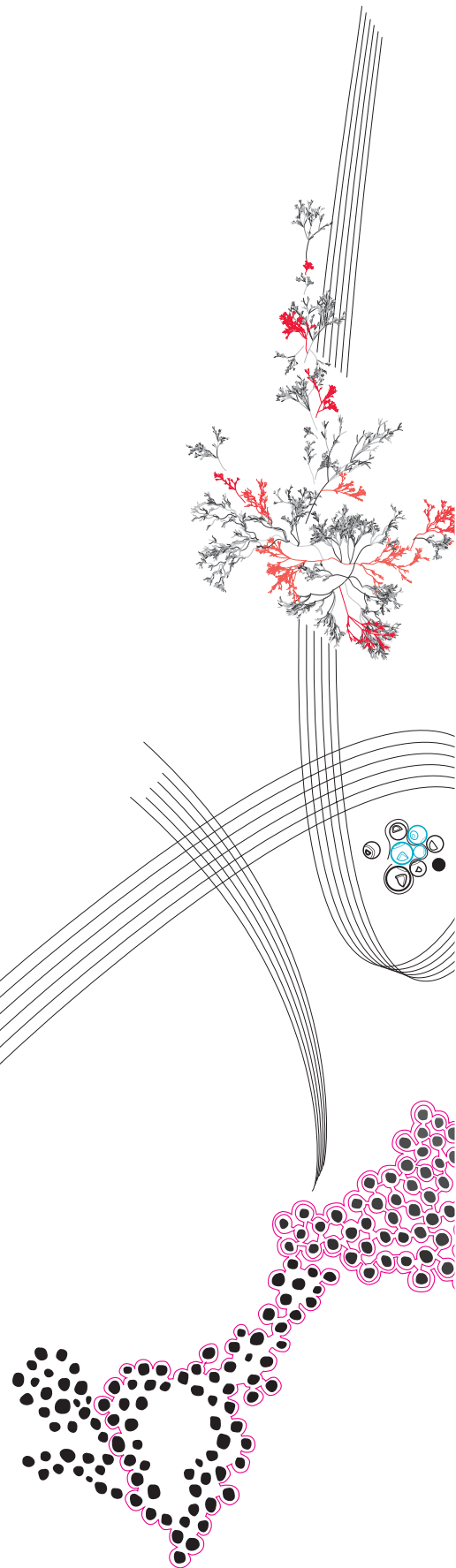
# On the speed characteristics of fault detection algorithms in dynamical systems

Sven Dummer

Supervisor: prof.dr. A.A. Stoorvogel

June, 2019

Department of Applied Mathematics  
Faculty of Electrical Engineering,  
Mathematics and Computer Science



## **Preface**

This paper is written as a bachelor assignment of Applied Mathematics at the University of Twente. This paper is mostly targeted at my fellow students in mathematics.

I would like to thank my supervisor Anton Stoorvogel for the meetings, discussions and feedback, especially during the difficult writing part, as well as the many times he has read through the article for improvements. Moreover, I want to thank my family for their support. Additionally, I want to thank Femke Boelens for reviewing my report and her mental support throughout the project.

# On the speed characteristics of fault detection algorithms in dynamical systems

Sven. C. Dummer\*

June, 2019

## Abstract

Detecting faults in systems is important, as the occurrence of faults may have drastic consequences. In this paper, complications with respect to analytical model-based fault detection algorithms using statistical techniques are investigated. Using a static problem in combination with Monte Carlo simulations and analytical properties of some test statistics, properties regarding hypothesis testing were investigated. Moreover, applying a Kalman filter based detection scheme in combination with discretised stochastic differential equations, simulations were done for a DC motor. It followed that there is a trade-off between the certainty that a fault is reliably detected, the probability of a false alarm and the speed of detection. Moreover, complications such as a dependency on both the sampling interval and the number of measurements per sample occurred. The dynamical case has many more complications to deal with than the static problem.

*Keywords:* Fault detection, FD, statistics, discretisation, dynamical systems, linear systems, Kalman filter, DC motor

## 1 Introduction

To maintain the reliability, safety and efficiency of systems, faults in the system must be detected. When a fault occurs, there can be several consequences. For instance, the system can become less efficient or the quality of the product the system makes can be reduced. In these cases, there are economic losses due to the fault. To reduce the total loss, it is necessary to quickly detect that a fault occurred. Furthermore, a fault can result in a complete breakdown of the process, which could have major consequences. If an important machine in a company breaks down completely, the production process could come to a halt, causing a significant loss of money. To prevent such a scenario, the fault should be detected.

Undetected faults can have fatal consequences, for example, in Boeing airplanes. These airplanes react to many signals via sensors. If a sensor breaks, this could have detrimental consequences. For instance, if the height meter breaks and returns values that make an airplane quickly react incorrectly, the plane could crash. In this case, it is of utmost importance that the fault be detected as quickly as possible.

Sensors are not the only apparatus in an airplane that can break down. On 4 October 1992, El Al Flight 1862 lost all its engines when departing from Schiphol Airport. Eventually, the pilot lost control and the plane crashed into two flats in the Bijlmermeer neighbourhood

---

\*Email: s.c.dummer@student.utwente.nl

of Amsterdam. Investigations showed that this incident, called 'Bijlmerramp' (Bijlmer disaster), could have been averted by rearranging the controller [1] [15].

This is not the only example of fatal consequences due to fault detection errors. American Airline flight DC10 crashed at Chicago-O'Hare International Airport with 273 fatalities. The pilot of the airplane only received an indication of a fault, 15 seconds before the accident. Investigations showed that the crash could have been averted [1].

Another such tragedy is the Chernobyl disaster in 1986, where a large explosion occurred in a nuclear power plant. The primary source of the Chernobyl disaster was the faulty obsolete technology and the absence of a fault handling mechanism [1].

The preceding examples indicate the importance of quick fault detection. The complexity of some systems, however, makes it hard to detect faults. Therefore, sophisticated fault detection methods should be created. In this paper, complications of fault detection methods were researched.

## 1.1 Literature review

According to Isermann [11], 'a fault is an unpermitted deviation of at least one characteristic property (feature) of the system from the acceptable, usual, standard condition'. A fault can occur as a result of internal or external sources. An example of an internal source is overheating, and an example of an external source is humidity.

Faults are unsatisfactory and need to be repaired. Fault diagnosis plays an important role in this process. As described by Ding [5], fault diagnosis consists of

- **Fault detection:** 'detection of the occurrence of faults in the functional units of the process, which lead to undesired or intolerable behaviour of the whole system'
- **Fault isolation:** 'localisation (classification) of different faults'
- **Fault analysis or fault identification:** 'determination of the type, magnitude and cause of the fault'

Fault detection is the first step in fault diagnosis. Fault detection includes two important tasks: residual generation and residual evaluation. The residual generation procedure creates signals that reflect the occurrence of faults. The residual evaluation procedure evaluates the residual signal to decide whether or not a fault has occurred.

According to Frank [8], fault detection techniques can be divided into the signal-based, analytical model-based and knowledge-based methods. In this paper, analytical model-based methods are considered. This class of methods uses a quantitative mathematical model to detect the occurrence of a fault. One such mathematical model is the dynamical system model. There are many analytical model-based fault detection techniques that use dynamical systems. Two general approaches are the parameter estimation technique and the observer technique [11] [1] [17] [10] [9] [5]. The model-based fault detection techniques are applied to many applications, such as robot manipulators [19] [3], aircraft [21] [2] and DC motors [18]. Fault detection algorithms may employ statistical techniques [5] and use a change in the statistical properties of the system to detect faults. Statistical techniques are used in, for instance, robot manipulators [19] and nuclear power plants [14].

## 1.2 Scope

The research performed so far is mostly concerned with whether the occurrence of a fault can be detected. Few books discuss why certain approaches fail to detect faults quickly. Nevertheless, this is important. For instance, a certain algorithm might only work in some situations. Investigating the properties and pinpointing the variables in the algorithm that

determine whether the algorithm can be used in a particular application of fault detection, can help determine whether the algorithm is suitable for that application or whether a different algorithm should be chosen. Moreover, pinpointing the reasons why a certain approach does not detect faults quickly, makes it possible to improve the algorithm (for that application).

Within this framework, this paper investigates complications regarding fault detection techniques that use the dynamical equation model and statistical techniques. The complications were investigated via a static problem and a Kalman filter fault detection technique. This paper focusses on fault detection methods applied in linear systems, as most researchers still use linear systems. For instance, linear systems can be used when the system dynamics are fluctuating around an equilibrium. In addition, the dynamical equations are often linearised around a trajectory. In this case, the deviations from the trajectory are considered. As linear models are ubiquitous, they are a natural choice to research.

### 1.3 Outline

First, some general terminology is defined in Chapter 2. Instead of immediately investigating linear models, a problem without dynamics is considered first in Chapter 3. Using this static problem, performance properties of test statistics are discussed. Subsequently, Chapter 4 introduces a linear model for a DC motor and describes a fault detection scheme that applies a Kalman filter. Using this fault detection scheme, Chapter 5 treats general complications regarding to the speed of a fault detection algorithm. Next, Chapter 6 discusses the results and Chapter 7 presents the conclusions.

## 2 Terminology

In this chapter, some standard terminology is introduced. Let  $x(i)$  denote measurement  $i$ . The sample mean is defined by

$$\bar{X} = \frac{1}{n} \sum_{i=1}^n x(i).$$

In addition, the sample variance is defined by

$$S^2 = \frac{1}{n-1} \sum_{i=1}^n (x(i) - \bar{X})^2.$$

Lastly,  $S_\mu^2$  is defined as

$$S_\mu^2 = \frac{1}{n} \sum_{i=1}^n (x(i) - \mu)^2.$$

Besides these notations, some concepts need to be introduced. If a null hypothesis  $H_0$  and an alternative hypothesis  $H_1$  are given, a type I error is the incorrect rejection of  $H_0$ . In other words, even though the null hypothesis  $H_0$  is true, it is rejected. A type II error is the incorrect acceptance of the null hypothesis. In other words, the null hypothesis  $H_0$  is accepted even though the alternative hypothesis  $H_1$  is true. The power of a statistical test is defined as the probability of correctly rejecting the null hypothesis. Hence, the power of a test equals  $P(\text{reject } H_0 | H_1 \text{ is true}) = 1 - P(\text{accept } H_0 | H_1 \text{ is true}) = 1 - P(\text{type II error})$ . Aside from statistical concepts and notations, faults can be classified as multiplicative and additive faults. Assume some output signal  $Y(t)$  and some input variable  $U(t)$  are present. If  $Y(t) = Y_u(t) + f(t)$ ,  $f(t)$  is an additive fault. If  $Y(t) = (a + \Delta a(t))U(t) = Y_u(t) + \Delta a(t)U(t)$ ,  $\Delta a(t)$  is a multiplicative fault. Additive faults may appear as offsets in a sensor. Examples of multiplicative faults are parameter changes in a specific process

[10].

### 3 Static problem

In this chapter, the following situation is treated. Assume measurements are performed from a normal distribution with mean  $\mu_1$  and variance  $\sigma_1^2$ . In this situation, a fault occurs when measurements are performed from a normally distributed random variable with mean  $\mu_2$  and  $\sigma_2^2$ . In this situation, the following questions were formulated:

- What is the relationship between power and the probability of errors of the first type? And does the power depend on the situation?
- Are comparisons based on power and fixed probability of errors of the first type fair? If not, what is a good replacement? And what are the differences?
- Are some test statistics better than others?
- How is the speed of detection related to power?

#### 3.1 Method

To answer these questions, simulations and analytical results were used. For simulation purposes, normally distributed measurements were generated. Different measurements from a specific distribution (either from  $\mathcal{N}(\mu_1, \sigma_1^2)$  or from  $\mathcal{N}(\mu_2, \sigma_2^2)$ ) are independent. The null hypothesis  $H_0$  applies when all measurements in the sample have been done from the  $\mathcal{N}(\mu_1, \sigma_1^2)$  distribution. The alternative hypothesis  $H_1$  applies when some of the measurements in the sample have been drawn from the  $\mathcal{N}(\mu_2, \sigma_2^2)$  distribution. These hypotheses were tested using basic statistics that is introduced later. For this purpose, samples were used, where  $n$  is defined as the number of measurements per sample. After a hypothesis test, more measurements were generated. If  $n$  new measurements were found, these new measurements formed a sample and were again used for hypothesis testing.

The used test statistics are  $Z = \frac{\bar{X} - \mu_1}{\sigma_1/\sqrt{n}}$ ,  $X_n^2 = \frac{nS_{\mu_1}^2}{\sigma_1^2}$ ,  $T = \frac{\bar{X} - \mu_1}{S/\sqrt{n}}$ ,  $X_{n-1}^2 = \frac{(n-1)S^2}{\sigma_1^2}$  and  $b_1\bar{X} + b_2S_{\mu_1}^2$  (called the summed test statistic). When no fault has occurred, the first four test statistics have an  $\mathcal{N}(0, 1)$ ,  $\chi_n^2$ ,  $t_{n-1}$  and  $\chi_{n-1}^2$  distribution, respectively [16]. The distribution of the summed test statistic is determined numerically using Monte-Carlo simulations. For our purposes,  $b_1 = b_2 = 1$  was used. Furthermore, it was assumed that it is not known whether the  $\mu_2$  and  $\sigma_2^2$  are larger or smaller than  $\mu_1$  and  $\sigma_1^2$ , respectively. As a consequence, two sides tests were used. If it was known that  $\mu_2$  and  $\sigma_2^2$  are larger or smaller than  $\mu_1$  and  $\sigma_1^2$ , respectively, a one sided test would have been preferred.

For the  $Z$  test statistic, the null hypothesis is rejected if  $Z > c$  or  $Z < -c$ . The parameter  $c$  depends on the choice of the level of confidence. The power of  $Z$  equals

$$1 - P(-c \leq Z \leq c | H_1) = 1 - P\left(\mu_1 - c \frac{\sigma_1}{\sqrt{n}} \leq \bar{X} \leq \mu_1 + c \frac{\sigma_1}{\sqrt{n}} | H_1\right)$$

The power can be calculated if all measurements in the batch are faulty since in this case,  $\bar{X} \sim \mathcal{N}(\mu_2, \frac{\sigma_2^2}{n})$ . If only  $k$  measurements in the batch are faulty, the situation is different. It can be shown that  $\bar{X} = \frac{n-k}{n}\bar{X}_{nf} + \frac{k}{n}\bar{X}_f$  with  $\bar{X}_{nf}$  the average of the nonfaulty measurements and  $\bar{X}_f$  the average of the faulty measurements. Using that  $\bar{X}_{nf} \sim \mathcal{N}(\mu_1, \frac{\sigma_1^2}{n-k})$  and  $\bar{X}_f \sim \mathcal{N}(\mu_2, \frac{\sigma_2^2}{k})$ , it follows that

$$\bar{X} \sim \mathcal{N}\left(\frac{(n-k)\mu_1 + k\mu_2}{n}, \frac{(n-k)\sigma_1^2 + k\sigma_2^2}{n^2}\right).$$

For the test statistic  $X_{n-1}^2$ , the power equals

$$1 - P(c_1 \leq X_{n-1}^2 \leq c_2 | H_1) = 1 - P\left(c_1 \frac{\sigma_1^2}{\sigma_2^2} \leq \frac{(n-1)S^2}{\sigma_2^2} \leq c_2 \frac{\sigma_1^2}{\sigma_2^2} | H_1\right).$$

When only faulty measurements are present in a batch,  $\frac{(n-1)S^2}{\sigma_2^2}$  has an  $\chi_{n-1}^2$  distribution.

As a consequence, the power can be calculated.

The preceding three facts were used in the analysis. When it is said that analytical results for  $Z$  or  $X_{n-1}^2$  were used, this means that one of the preceding facts was used to perform an analysis. Which fact was used is clear from the context.

### 3.2 The relation between power and errors of the first type and properties of the power

In this section, the relation between power and the probability of errors of the first type, is investigated using analytical results and simulations. In addition, properties of the power are discussed.

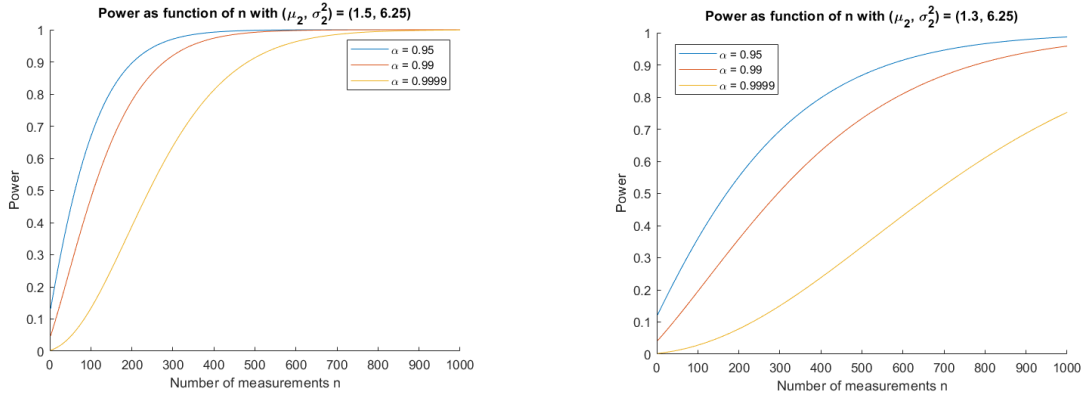
#### 3.2.1 A comment regarding differences in test statistics

Before moving on to the relation between the power and the probability of type I errors, a property of the test statistics is discussed. Assume that all measurements in a sample are faulty measurements. The  $Z$  test statistic assumes the variance to be known, while the  $T$  test statistic estimates the variance. Hence, if the variance changes and there are sufficiently many measurements in a sample, the  $T$  test statistic approximates the variance well and can not see the change in the variance. As a consequence, the test statistic  $T$  can only detect changes in the mean. The  $Z$  test statistic does not adjust to the change in the variance which implies that the  $Z$  test statistic could detect changes in both the mean and the variance. Hence, if the variance changes, the power of the two test statistics may differ. If the variance stays the same and the number of measurements per sample is large enough,  $S$  estimates the variance very well and the  $Z$  and  $T$  test statistic most likely behave approximately the same way.

Applying a similar story to  $X_n^2$  and  $X_{n-1}^2$ , if the mean changes,  $X_n^2$  does not adapt to this change and  $X_{n-1}^2$  does. As a consequence,  $X_n^2$  can detect changes in both the mean and the variance, while  $X_{n-1}^2$  can only detect changes in the variance. In this case, the power of both test statistics may differ. If the mean does not change and the sample size is large enough,  $\bar{X}$  approximates the mean well and  $X_{n-1}^2$  and  $X_n^2$  behave approximately the same way.

#### 3.2.2 A change for all measurements in the sample

In this subsection, the relation between power and the probability of errors of the first type is investigated for the case that faults are present in all the measurements of the sample. The analytical results for the  $Z$  test statistic are presented in Figure 1.



(A)  $(\mu_1, \sigma_1^2) = (1, 4)$  and  $(\mu_2, \sigma_2^2) = (1.5, 6.25)$ .  
(B)  $(\mu_1, \sigma_1^2) = (1, 4)$  and  $(\mu_2, \sigma_2^2) = (1.3, 6.25)$ .

FIGURE 1: The power of the test statistic  $Z$  as a function of the number of measurements per sample for different probabilities of a type I error  $\alpha$ . Two scenarios are treated.

Figure 1 shows that the power increases as the number of measurements increases. In addition, the larger the difference between  $\mu_1$  and  $\mu_2$ , the faster the power converges to 1. Simulations showed that these properties of power hold for  $T$  and  $X_n^2$ . The analytical results for  $X_{n-1}^2$  showed the same behaviour as well.

While performing the simulations, another property of the  $Z$  and  $T$  test statistic was found. It is known that the test statistics  $Z$  and  $T$  are designed to detect changes in the mean. For these test statistics, the magnitude of the variance plays a role in the power as well. If the variance is larger, the power is smaller for the same change of  $\mu_1$  to  $\mu_2$ . This phenomenon can be seen in Figure 13 in Appendix E. This figure is generated by using the analytical results for the  $Z$  test statistic.

The reason for this phenomenon is simple. For instance, for  $Z$ , the null hypothesis is rejected if  $\bar{X}$  lies outside  $(\mu_1 - c\frac{\sigma_1}{\sqrt{n}}, \mu_1 + c\frac{\sigma_1}{\sqrt{n}})$ . When a fault has occurred,  $\bar{X}$  is normally distributed with mean  $\mu_2$  and variance  $\frac{\sigma_2^2}{n}$ . If  $\sigma_1$  is large,  $\mu_2$  may lie inside this interval. In this case, due to symmetry of the normal distribution, the probability is large that  $\bar{X}$  is again in  $(\mu_1 - c\frac{\sigma_1}{\sqrt{n}}, \mu_1 + c\frac{\sigma_1}{\sqrt{n}})$ . If  $\mu_2$  lies outside the interval, a large  $\sigma_2$  can cause problems. A large  $\sigma_2$  may cause  $\bar{X}$  to have a high probability to be in  $(\mu_1 - c\frac{\sigma_1}{\sqrt{n}}, \mu_1 + c\frac{\sigma_1}{\sqrt{n}})$ . In such situations, the power is much lower. Replacing  $\sigma_1$  by  $S$ , the same conclusion is obtained for  $T$  when  $n$  is sufficiently large.

Additionally, in Figure 13, the variance does not change after the fault. As mentioned in Subsection 3.2.1, it is expected that the  $Z$  and  $T$  test statistics behave approximately the same way in terms of power.

### 3.2.3 Trade-off

Figure 1 indicates a trade-off. Given a value of  $n$  either the probability of a type I error and the power are increased or both are decreased. One possibility to decrease the probability of a type I error and increase the power, is to increase  $n$ . This phenomenon is more accurately represented in Figure 2 for the test statistic  $Z$ . For this figure, all measurements in the samples are faulty. The corresponding analytical result for  $Z$  was used to generate the figure.

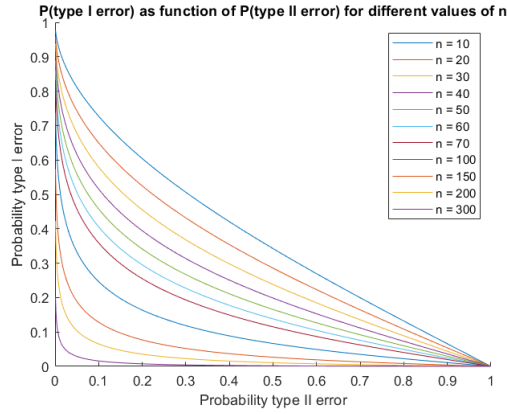


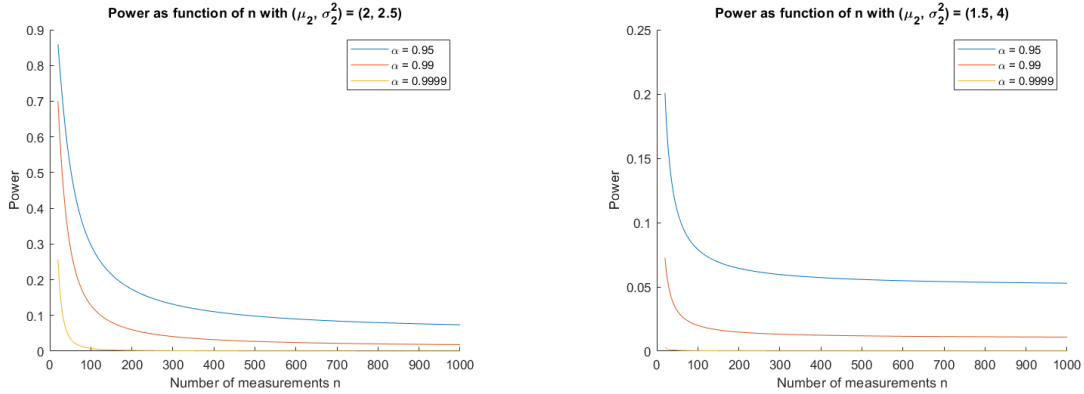
FIGURE 2: Probability of type I error against probability of type II error for different values of  $n$  using the  $Z$  test statistic. The values  $(\mu_1, \sigma_1^2) = (1, 4)$  and  $(\mu_2, \sigma_2^2) = (1.5, 6.25)$  were taken.

A high power and a low probability of a type I error is desired, however, not at all costs. If too large an  $n$  is chosen, the detection of the fault will take a very long time. If a measurements is performed every 0.1 seconds and a fault needs to be detected within 10 seconds, choosing an  $n$  larger than 100 is not desirable. In this sense, not only is there a trade off between the power and the probability of a type I error, there is a trade-off between certainty and detection speed as well.

Some types of faults need to be detected quickly. For instance, if a fault in an airplane occurs, the airplane can crash if the fault is not detected quickly. For faults that have to be detected quickly,  $n$  cannot be too large. Figure 2 shows that when faults have to be detected quickly to prevent bad consequences a lower level of confidence is acceptable to achieve a higher power. When faults do not have to be detected quickly and only produce unacceptable consequences when present for a relatively long time, a higher level of confidence and a lower power can be used, as well as a higher value for  $n$ .

### 3.2.4 A change for a part of the measurements in the sample

As in the previous subsection, the power is considered here. However, a different situation is treated. A fault could be measurable only for a short time after the fault occurred. As a consequence, only a small number of faulty measurements are available, and they need to be used efficiently. With respect to this application, the results in this subsection assume that only a fixed number of faults occur in a specific batch. For the analysis, samples with at least 20 measurements were considered. The simulations for  $T$ ,  $X_n^2$  and  $X_{n-1}^2$  and the analytical results for  $Z$  were obtained by assuming that only 20 faulty measurements are present in each batch. Analytical results regarding the  $Z$  test statistic are presented in Figure 3. Similar results hold for the other test statistics.



(A)  $(\mu_1, \sigma_1^2) = (1, 2)$  and  $(\mu_2, \sigma_2^2) = (2, 2.5)$ . (B)  $(\mu_1, \sigma_1^2) = (1, 4)$  and  $(\mu_2, \sigma_2^2) = (1.5, 4)$ .

FIGURE 3: The power of the test statistic  $Z$  as a function of the number of measurements per sample for different probabilities of a type I error  $\alpha$ . Two scenarios are treated.

Figure 3 shows that the bigger the fraction of measurements that are faulty, the higher the power. In the simulations for  $T$ ,  $X_n^2$  and  $X_{n-1}^2$ , almost all the outcomes resembled Figure 3. However, performing a simulation of a specific fault scenario for the  $X_{n-1}^2$  test statistic, a different graph occurred. This scenario uses a 95% confidence level and is depicted in Figure 4.

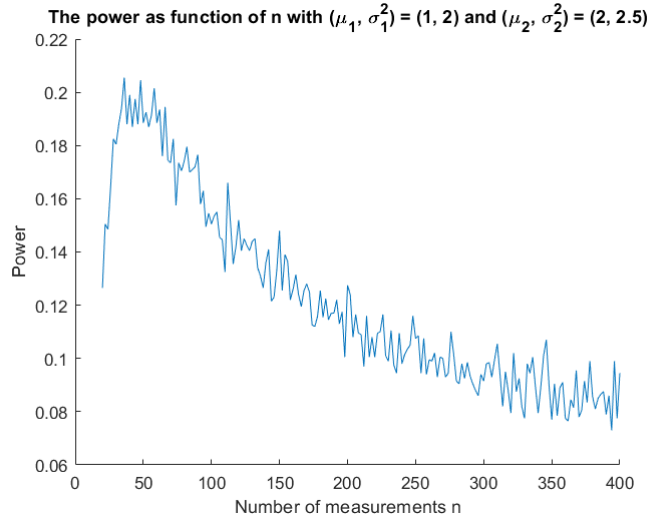


FIGURE 4: Power as a function of the number of measurements for the  $X_{n-1}^2$  test statistic under a specific fault, using a confidence level of 95%.

The difference between Figures 3 and 4 is that at the start of Figure 4, the (estimated) power increases instead of decreases. Although there are contrasts between Figures 3 and 4, the two figures demonstrate that the power diminishes when the number of measurements is significantly large. All in all, it can be concluded that for a constant deviation from the normal value occurring only 20 consecutive measurements in only one specific batch, it might be sensible to take the number of measurements per sample  $n$  equal to 20. If this is not possible, one should take as many faulty measurements as possible. However, this does not apply to every situation.

Moreover, the trade-off between the probability of a type I error and the power is visible in Figure 3. The larger the probability of a type I error, the smaller the power and vice versa.

### 3.3 Confidence levels depending on the number of measurements per batch

Comparisons between different values of  $n$  with a fixed confidence level not depending on  $n$ , might not be fair. Assume that measurements are performed every 0.01 seconds, batches are used with  $n$  measurements and a confidence level of  $\alpha = 95\%$  is used. For  $n = 10$ , a false alarm occurs on average every 2 seconds. For  $n = 1000$ , a false alarm occurs on average every 200 seconds. In this sense, the two tests are not comparable in a fair way. In this section, a test is designed to ensure a fixed average number of false alarms in a given time interval.

For now, an average of 1 false alarm every 120 seconds is used. Moreover, measurements are performed every 0.1 seconds. The number of batches in 120 seconds is  $n_b(n) = \frac{120}{0.1n} = \frac{1200}{n}$ . The test statistic  $Y$  is chosen such that it only depends on the measurements in a specific batch. Due to independent measurements, the batches are independent. As a consequence, the values of  $Y$  of different batches are independent.

Let  $p(n) = P(Y \leq c_1(n) \text{ OR } Y \geq c_2(n) | H_0)$  be the probability of a type I error. Assume we have  $n$  batches numbered  $(1, 2, \dots, n)$ . Here  $H_0$  is 'no fault occurred in batch  $i$  and in batch  $j$  ( $j \in (1, 2, 3, \dots, i - 1)$ )'. The alternative hypothesis  $H_1$  is that the null hypothesis  $H_0$  is false. The probability of rejecting the null hypothesis incorrectly exactly  $i$  times is binomially distributed with number of trials  $n_b(n)$  and probability  $p(n)$ . If we want only 1 false alarm in 120 seconds,  $n_b(n) \cdot p(n) = 1$ . In other words,  $P(Y \leq c_1(n) \text{ OR } Y \geq c_2(n) | H_0) = p(n) = \frac{1}{n_b} = \frac{n}{1200}$ . Hence, given  $n$ ,  $c_1(n)$  and  $c_2(n)$  can be determined such that  $P(Y \leq c_1(n) \text{ OR } Y \geq c_2(n) | H_0) = \frac{n}{1200}$ . In this way, a test has been constructed such that on average 1 false alarm occurs in 120 seconds. When this scheme is applied, it will be said that adaptive confidence levels are used. In this case, both the probability of a type I and type II error (and the confidence intervals used to determine them) depend on the number of measurements per sample  $n$ .

Using adaptive confidence levels, the power was investigated. To conduct the investigation, it is assumed that measurements are performed every 0.1 seconds. For the case where only 20 faulty measurements are present in a specific batch, an adaptive confidence level is used with an average of 1 false alarm every 120 seconds. For this scenario, the power was investigated using analytical results and simulations. The analytical results for the  $Z$  statistic are shown in Figure 5. This figure represents the power of the  $Z$  test statistic when a batch contains  $n \geq 20$  measurements and where only 20 of the  $n$  measurements are faulty.

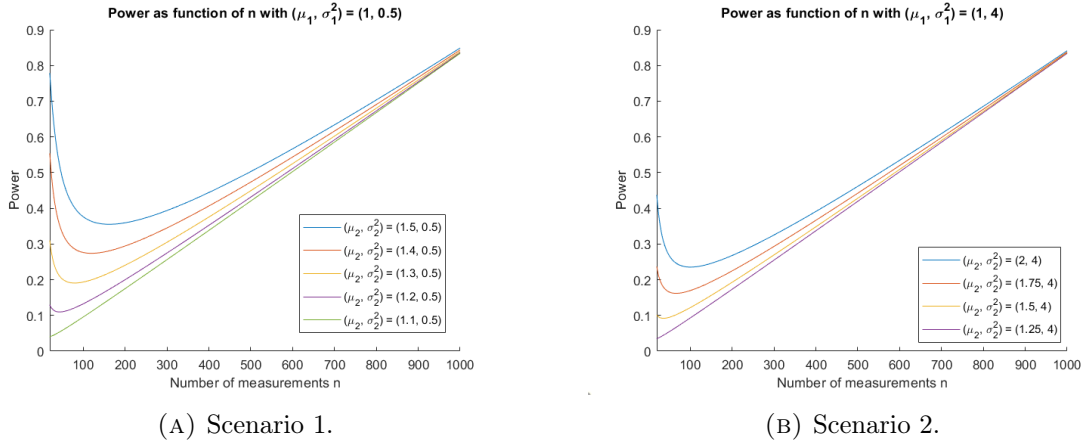


FIGURE 5: The power of the  $Z$  test statistic when  $n$  measurements from a specific batch are used and where only 20 out of the  $n$  measurements are faulty. Two scenarios are treated.

The simulated results for the  $X_n^2$  and the summed test statistic when  $(\mu_1, \sigma_1^2) = (1, 4)$  show similar behaviour to Figure 5 in case of only an increase in the variance and an increase in both the variance and the mean, respectively. The difference between Figures 3 and 5 is clear. Instead of tending to zero, the power starts to increase from a certain value of  $n$ . This is due to the (adaptive) confidence level tending to zero as  $n$  tends to 1200.

If instead of once every 120 seconds, a false alarm occurs on average once every day, then  $p(n) = \frac{864000}{n}$  and the effect of the previously discussed phenomenon is limited. This decreases the probability of a type I error significantly. As mentioned in Section 3.2, this means the power decreases significantly as well. As discussed in Subsection 3.2.3, the choices made in this trade-off between these two quantities, depend on the application. Furthermore, for the scenario where all the measurements in a batch are faulty, the consequence of using the adaptive confidence level is easily seen. Due to the increase of the probability of a type I error, the power increases more than when the probability of a type I error is the same for every  $n$ .

### 3.4 Comparing test statistics

Using adaptive confidence levels, the test statistics were compared for the scenario, as described in Subsection 3.2.2. Given that measurements were performed every 0.1 seconds, the adaptive confidence level was chosen such that 1 false alarm occurred on average every 120 seconds. The results for the difference between the power of  $Z$  and  $T$  are presented in Figure 20a in Appendix E. Some results for the difference in power between the summed test statistic and the maximum power of  $Z$  and  $X_n^2$ , are shown in Figure 20b in Appendix E. Similar simulations were done for the comparison between  $X_n^2$  and  $X_{n-1}^2$ . The power of  $Z$  and  $X_{n-1}^2$  was calculated using analytical results. The power of  $T$ ,  $X_n^2$  and the summed test statistic was estimated using simulations. For some of these comparisons, it was assumed that  $\mu_2 \geq \mu_1$  and  $\sigma_2^2 \geq \sigma_1^2$ . These comparisons between  $Z$  and  $T$  and between  $X_n^2$  and  $X_{n-1}^2$  show that  $Z$  and  $X_n^2$  are superior in terms of power (for the performed simulations). There is only one situation in which  $Z$  and  $X_n^2$  are comparable to  $T$  and  $X_{n-1}^2$ , respectively. For  $Z$  and  $T$ , this is when only the mean changes. On the other hand, for  $X_n^2$  and  $X_{n-1}^2$ , this occurs when only  $\sigma_1^2$  changes. Nevertheless, when the variance decreases, the  $T$  test statistic has higher power. Furthermore, using  $(\mu_1, \sigma_1^2) = (1, 4)$  and  $(\mu_2, \sigma_2^2) = (1.5, 3.0625)$  together with simulations of  $X_n^2$  and analytical results of  $X_{n-1}^2$ , it followed that the  $X_{n-1}^2$

test statistic outperforms  $X_n^2$  in terms of power. Some explanations for the phenomena seen, are given.

It can easily be shown that the statistics  $T$  and  $Z$  satisfy

$$T = \frac{\bar{X} - \mu_2}{S/\sqrt{n}} + \frac{\mu_2 - \mu_1}{S/\sqrt{n}},$$

$$Z = \frac{\sigma_2}{\sigma_1} \left( \frac{\bar{X} - \mu_2}{\sigma_2/\sqrt{n}} + \frac{\mu_2 - \mu_1}{\sigma_2/\sqrt{n}} \right) \sim \mathcal{N} \left( \left( \frac{\mu_2 - \mu_1}{\sigma_1/\sqrt{n}} \right), \left( \frac{\sigma_2}{\sigma_1} \right)^2 \right). \quad (1)$$

It is expected that for sufficiently large  $n$ ,  $S$  estimates  $\sigma_2$  very well. Combining this with Equation (1), it is expected that  $Z$  and  $T$  behave approximately the same if  $\sigma_2^2 = \sigma_1^2$ . In order to investigate whether this reasoning is correct, simulations and analytical results with the same confidence levels for all  $n$ , were used. The 95%, 99% and 99.99% confidence levels were used. Using simulations for  $T$  and using analytical results for  $Z$  with  $(\mu_1, \sigma_1^2) = (1, 0.5)$  and  $(\mu_2, \sigma_2^2) = (1.5, 0.5)$ , the power of the  $Z$  test statistic, in general, is higher than the estimated power of the  $T$  test statistic for  $n = 10, 20, 30, \dots, 90$ . When the  $T$  test statistic had higher values, the differences were only very small and could be due to estimation errors. It is not clear to us why  $Z$  is better than  $T$  in this scenario. It is expected it has something to do with the skewness of the distribution of  $S$ . This could be further investigated.

Now the situation  $\sigma_2^2 > \sigma_1^2$  is treated. For the  $Z$  statistic the confidence interval is  $(-c_z, c_z)$  and for  $T$  it is  $(-c_t, c_t)$ . It is expected that  $\frac{\bar{X} - \mu_2}{S/\sqrt{n}} + \frac{\mu_2 - \mu_1}{S/\sqrt{n}}$  is not significantly different from  $\left( \frac{\bar{X} - \mu_2}{\sigma_2/\sqrt{n}} + \frac{\mu_2 - \mu_1}{\sigma_2/\sqrt{n}} \right)$  as  $S$  approximates  $\sigma_2$ . If  $\sigma_2^2 > \sigma_1^2$ ,  $\frac{\sigma_2}{\sigma_1} > 1$ . Using equation (1), if  $T = \frac{\bar{X} - \mu_2}{S/\sqrt{n}} + \frac{\mu_2 - \mu_1}{S/\sqrt{n}}$  is not significantly different from  $\left( \frac{\bar{X} - \mu_2}{\sigma_2/\sqrt{n}} + \frac{\mu_2 - \mu_1}{\sigma_2/\sqrt{n}} \right)$ , it is likely that  $Z$  is larger in magnitude than  $T$  due to  $\frac{\sigma_2}{\sigma_1} > 1$ . As the confidence intervals are symmetric around zero,  $Z$  most likely has a higher probability than  $T$  to fall outside their respective confidence intervals. As a consequence,  $Z$  most likely performs better than  $T$ . This may be the reason why  $Z$  has a higher power than  $T$  when  $(\mu_1, \sigma_1^2) = (1, 4)$  and  $(\mu_2, \sigma_2^2) = (1.5, 6.25)$ .

On the other hand, if  $\sigma_2^2 < \sigma_1^2$ , the magnitude of  $Z$  is most likely closer to zero than  $T$  as  $\frac{\bar{X} - \mu_2}{S/\sqrt{n}} + \frac{\mu_2 - \mu_1}{S/\sqrt{n}}$  is expected to not be significantly different from  $\left( \frac{\bar{X} - \mu_2}{\sigma_2/\sqrt{n}} + \frac{\mu_2 - \mu_1}{\sigma_2/\sqrt{n}} \right)$  and  $\frac{\sigma_2}{\sigma_1} < 1$ . This implies that it could be more likely for  $Z$  to fall in  $(-c_z, c_z)$  than  $T$  to fall in  $(-c_t, c_t)$ . As a consequence,  $T$  has a higher power than  $Z$ . This explains why  $T$  has higher power than  $Z$  when  $(\mu_1, \sigma_1^2) = (1, 4)$  and  $(\mu_2, \sigma_2^2) = (1.5, 2.25)$ .

Having treated the test statistics  $Z$  and  $T$ , the test statistics  $X_n^2$  and  $X_{n-1}^2$  are treated. Using  $nS_{\mu_1}^2 = \sum_{i=1}^n (X_i - \mu_1)^2$  with  $\mu_1 = \mu_2 + \mu_1 - \mu_2$ , it can easily be shown that

$$X_n^2 = \frac{nS_{\mu_1}^2}{\sigma_1^2} = \frac{\sigma_2^2}{\sigma_1^2} \left( \frac{nS_{\mu_2}^2}{\sigma_2^2} + \frac{2n(\mu_2 - \mu_1)(\bar{X} - \mu_2) + n(\mu_2 - \mu_1)^2}{\sigma_2^2} \right) \quad (2)$$

$$X_{n-1}^2 = \frac{(n-1)S^2}{\sigma_1^2} = \frac{\sigma_2^2}{\sigma_1^2} \left( \frac{(n-1)S^2}{\sigma_2^2} \right). \quad (3)$$

It is expected that  $X_n^2$  and  $X_{n-1}^2$  behave approximately the same when  $\mu_2 = \mu_1$  as then it is conjectured that  $\frac{nS_{\mu_2}^2}{\sigma_2^2} \approx \frac{(n-1)S^2}{\sigma_2^2}$  due to the fact that  $\bar{X}$  approximates  $\mu_2$  very well and the remainder term in Equation (2) is not present. Such intuition does not seem to apply when comparing  $Z$  and  $T$ . Hence, it might not apply to  $X_n^2$  and  $X_{n-1}^2$  either. However, we have not found a counterexample. As a consequence, it is not certain whether the intuition is false. This could be investigated more thoroughly.

If the values of  $\frac{nS_{\mu_2}^2}{\sigma_2^2}$  and  $\frac{(n-1)S^2}{\sigma_2^2}$  are not significantly different,  $\frac{2n(\mu_2 - \mu_1)(\bar{X} - \mu_2) + n(\mu_2 - \mu_1)^2}{\sigma_2^2}$  is

the main term that determines the difference in power. Given a  $\sigma_1^2$ ,  $\sigma_2^2$  and  $\mu_1$ , this term is mainly governed by the choice of  $\mu_2$ . By suitably adjusting  $\mu_2$ , the magnitude of the term can be influenced. Assume  $\sigma_2^2 > \sigma_1^2$ . When  $\mu_2 \neq 0$ ,  $\frac{2n(\mu_2 - \mu_1)(\bar{X} - \mu_2) + n(\mu_2 - \mu_1)^2}{\sigma_2^2}$  is on average larger than zero. Combining this with the increase in the variance,  $X_n^2$  is more likely to fall outside the right bound of the confidence interval than when only the variance changes. The statistic  $X_{n-1}^2$  is not influenced by  $\mu_2$ . As a consequence,  $X_{n-1}^2$  most likely performs worse than  $X_n^2$ . This is most likely the reason that  $X_n^2$  performed better for  $\sigma_2^2 \geq \sigma_1^2$  and  $\mu_2 \geq \mu_1$ . If  $\sigma_2^2 < \sigma_1^2$ ,  $\frac{\sigma_2^2 n S_{\mu_2}^2}{\sigma_1^2}$  is more likely to exceed the left bound of the confidence level than the right bound. By choosing  $\mu_2$  appropriately,  $\frac{2n(\mu_2 - \mu_1)(\bar{X} - \mu_2) + n(\mu_2 - \mu_1)^2}{\sigma_2^2}$  can be given an average value such that it is more likely for  $X_n^2$  to be inside the confidence interval. As  $X_{n-1}^2$  is not influenced by  $\mu_2$ ,  $X_{n-1}^2$  most likely performs better in this situation. It is very probable that this occurred when  $(\mu_1, \sigma_1^2) = (1, 4)$  and  $(\mu_2, \sigma_2^2) = (1.5, 3.0625)$ . Regarding the summed test statistic, similar phenomena can be seen in Figure 20b in Appendix E. A possible reason for the presence of one phenomenon is now discussed. Assume that when a fault occurs,  $(\mu_1, \sigma_1^2) = (1, 4)$  changes to  $(\mu_2, \sigma_2^2) = (1.5, 2.3^2)$ . In this scenario, the graphs of the power of both  $Z$  and  $X_n^2$  as functions of  $n$  were close together. Figure 20b in Appendix E implies that the summed test statistic is the best in this scenario. Additionally, it shows that when only the mean or only the variance increases, it is better to just use  $Z$  or  $X_n^2$ , respectively. Generalizing, it could be that when both the mean and variance change in a certain manner such that the power of  $Z$  and  $X_n^2$  are approximately equal, the summation of the two test statistics has a higher power. In the scenario that one has a considerably larger power, it may be better to use that particular test statistic. Furthermore, the optimal coefficients  $b_1$  and  $b_2$  most likely depend on the changes in  $\mu_1$  and  $\sigma_1$ . When  $(\mu_1, \sigma_1^2) = (1, 4)$  changes to  $(\mu_2, \sigma_2^2) = (1.5, 2.3^2)$ , the power of  $Z$  and  $X_n^2$  are deterministic. If  $\mu_1$  would have changed more than 0.5 and  $\sigma_1$  less than 0.3, the power of  $Z$  may increase and the power of  $X_n^2$  may decrease. In this case, it may be more desirable to put a higher weight on  $Z$  than in the case that  $\mu_1$  increases with 0.5 and  $\sigma_1$  increases by 0.3.

### 3.5 Speed of detection

In the previous sections, the only point of discussion is the power. However, the power itself is not necessarily the most important quantity in fault detection. For the situation described in Subsection 3.2.4, the power is sufficient. However, for the situation described in Subsection 3.2.2 and using an adaptive confidence level, the time it takes until the fault is detected is more important. The significance of the power is its relationship with this time. For investigating the time it takes until the fault is detected, it was assumed that an infinite number of batches containing only faulty measurements are available. These batches were treated consecutively.

The number of batches needed to first reject the null hypothesis, is related to the speed of detection. By our assumptions, the number of batches needed to reject the null hypothesis for the first time  $N_s(n)$  is geometrically distributed with parameter equal to the power  $p_w(n, \alpha)$  when  $n$  measurements are used and a confidence level of  $\alpha$  is given. Hence, the expected number of measurements needed to reject the null hypothesis for the first time equals  $s_d = \frac{n}{p_w(n, \alpha)}$ .

If measurements are performed every 0.1 seconds, this means that it takes on average  $0.1s_d$  seconds to detect a specific fault. As a consequence, the smaller the  $s_d$ , the smaller the expected time until detection. Therefore,  $s_d$  should be as small as possible. The variance

of the time until detection is not really important. To see this, consider the case that the probability of a type I error is designed such that 1 false alarm occurs on average every 120 seconds, measurements are done every 0.1 seconds and for some value of  $n$ ,  $s_d = 200$ . Either many times a fault is detected with less than 200 measurements or not. If this does occur a lot, everything is fine. If this does not occur a lot, the other values must be very close to  $s_d = 200$  as else the average does not equal 200. Hence, the variance does not really provide new interesting information. Values such as  $s_d = 800$  are not wanted. The reason is that when no fault occurred, false alarms are already given every 1200 measurements. This is not really an improvement and hence not really interesting to look at. From the preceding considerations, it can be inferred that the variance is not really interesting to consider.

Figure 6 presents  $s_d$  for the  $Z$  test statistic in several fault scenarios and using an adaptive confidence level such that 1 false alarm occurs on average every 120 seconds. The figure was generated using the formula for  $s_d$  in combination with the analytical results for  $Z$ .

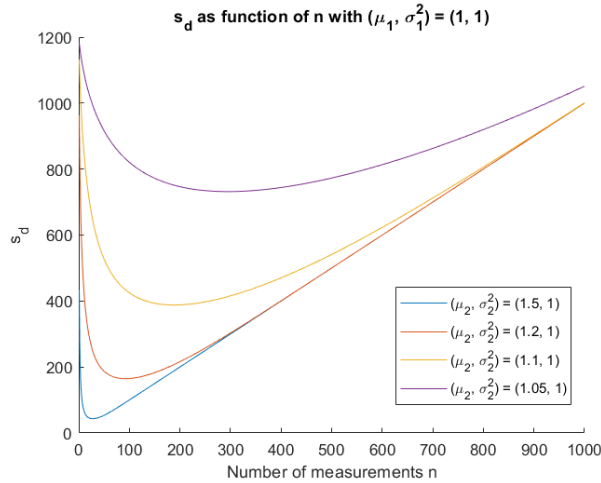


FIGURE 6: For the  $Z$  test statistic,  $s_d$  is plotted against the number of measurements per sample  $n$  with an adaptive confidence level such that 1 false alarm occurs on average every 120 seconds.

Depending on the fault situation, the graph in Figure 6 may turn out different. Figure 6 nicely illustrates the trade-off between the probability of a type I error, the power and the speed of detection. First, the probability of a type I error is fixed for each  $n$ . This depends on the choice in the trade-off between power and the probability of a type I error. As the probability of a type I error is fixed, the power as a function of  $n$  is deterministic. The power can be increased by choosing more measurements per sample. As Figure 6 shows, this can be detrimental for the speed until detection. This is the trade-off between more certainty to detect a fault against the speed it takes to detect the fault.

## 4 An application of fault detection to linear systems

Now that the static problem is discussed, a more complicated situation is treated. In this chapter, a fault detection approach for linear dynamical systems is discussed. For this discussion, some assumptions and a test system (a DC motor) are introduced.

## 4.1 Simulation equations

In this subsection, the dynamical equations of the DC motor are introduced. Furthermore, how faults, disturbances and (measurement) noise can be incorporated into linear models is discussed. Subsequently, the discretisation of the resulting models is considered.

### 4.1.1 Differential equations DC motor

A model of the dynamics of the Direct Current motor is given by

$$\begin{bmatrix} \dot{I} \\ \dot{\omega} \end{bmatrix} = \begin{bmatrix} -\frac{R}{L} & -\frac{k_m}{J} \\ \frac{k_m}{J} & -\frac{D_v}{J} \end{bmatrix} \begin{bmatrix} I \\ \omega \end{bmatrix} + \begin{bmatrix} \frac{1}{L} & 0 \\ 0 & -\frac{1}{J} \end{bmatrix} \begin{bmatrix} U \\ T_l \end{bmatrix}, \quad (4)$$

where  $I$  is the current in the motor,  $U$  is the input voltage to the motor,  $L$  is the self inductance of the coil in the motor,  $R$  is the resistance in the coils,  $k_m$  is the motor constant of the motor,  $J$  is the inertia of the rotor/load,  $D_v$  is a viscous friction coefficient (due to the rotation of the rotor) and  $T_l$  is a load torque disturbance. For a derivation of the equations, see Krishnan [13]. The output of the system is assumed to be

$$y = C \begin{bmatrix} I \\ \omega \end{bmatrix} \quad (5)$$

for some matrix  $C$  of appropriate dimensions.

### 4.1.2 Modelling faults, disturbances and noise and discretising the continuous model

The overarching topic of this paper is fault detection. Hence, the models need to incorporate faulty behaviour. Furthermore, systems are almost always subject to process disturbance and (measurement) noise, so these phenomena need to be included in the model as well. For our purposes, the effects described above can be included by adapting the general linear system  $\dot{x}(t) = Ax(t) + Bu(t)$  to

$$\begin{aligned} \dot{x}(t) &= (A + A_f(t))x(t) + (B + B_f(t))u(t) + E_f f_1(t) + E_w w(t) \\ &= \bar{A}(t)x(t) + \bar{B}(t)u(t) + E_f f_1(t) + E_w w(t) \end{aligned} \quad (6)$$

and adapting the output  $y(t) = Cx(t)$  to

$$y(t) = Cx(t) + F_f f_2(t) + v(t). \quad (7)$$

Here  $w$  and  $v$  are stochastic processes representing disturbances in the system and noise in the sensor, respectively,  $E_f$  and  $F_f$  are some known matrices, the vectors  $f_1$  and  $f_2$  are additive fault vectors, and the matrices  $A_f$  and  $B_f$  represent multiplicative faults.

Instead of the continuous differential Equations (6) and (7), discrete (difference) equations can be used. For the discretisation, let  $\Delta t$  be the time between state values. Assume that when  $x(k)$  is used, it means  $x(t)$  for  $t = k\Delta t$ . Replacing the derivative in  $\dot{x}(t)$  by the estimate  $\frac{x(t+\Delta t) - x(t)}{\Delta t}$  and manipulating the resulting equation yields

$$\begin{aligned} x(k+1) &= \bar{A}_d(k)x(k) + \bar{B}_d(k)u(k) + E_{d,f}f_1(k) + E_{d,w}w(k) \\ y(k) &= Cx(k) + F_f f_2(k) + v(k), \end{aligned} \quad (8)$$

where the matrices are given by

$$\bar{A}_d(k) = I + \Delta t A + \Delta t A_f(k), \quad \bar{B}_d = \Delta t B + \Delta t B_f(k), \quad E_{d,f} = \Delta t E_f, \quad E_{d,w} = \Delta t E_w. \quad (9)$$

Equations (8) and (9) form a good approximation when  $\Delta t$  is sufficiently small. A more accurate approach can be used, however. A system  $\dot{x}(t) = \bar{A}(t)x(t) + \bar{B}(t)u(t) + E_f f_1(t) + E_w \eta(t)$  is given with a stochastic process  $\eta(t)$  and piecewise continuous matrices  $\bar{A}(t)$  and  $\bar{B}(t)$ . Consider the integral version  $x(t) - x(0) = \int_0^t A(s)x(s)ds + \int_0^t B(s)u(s)ds + \int_0^t E_f f_1(s)ds + \int_0^t E_w \eta(s)ds$  of the differential equation. If we let  $\eta(t)$  formally be the derivative of a standard Brownian motion process  $\{w_t\}$ , then the last term can be replaced

by the Wiener integral  $\int_0^t E_w dw_\tau$ . The solution of the resulting equation is

$$\begin{aligned} x(t + \Delta t) = & \Phi(t + \Delta t, t)x(t) + \int_t^{t+\Delta t} \Phi(t + \Delta t, \tau)\bar{B}(\tau)u(\tau)d\tau \\ & + \int_t^{t+\Delta t} \Phi(t + \Delta t, \tau)E_f f_1(\tau)d\tau + \int_t^{t+\Delta t} \Phi(t + \Delta t, \tau)E_w dw_\tau, \end{aligned} \quad (10)$$

where the state transition matrix  $\Phi(t, \tau)$  satisfies

$$\begin{aligned} \frac{d\Phi(t, \tau)}{dt} &= \bar{A}(t)\Phi(t, \tau) \\ \Phi(\tau, \tau) &= I. \end{aligned}$$

In order to put Equation (10) into the form of Equation (8), the input is assumed to be either constant or generated using the zero order hold principle. Defining  $\bar{f}_1(t)$  and  $\bar{w}(t)$  as

$$\begin{aligned} \bar{f}_1(t) &= \int_t^{t+\Delta t} \Phi(t + \Delta t, \tau)E_f f_1(\tau)d\tau \\ \bar{w}(t) &= \int_t^{t+\Delta t} \Phi(t + \Delta t, \tau)E_w dw_\tau, \end{aligned} \quad (11)$$

Equation (10) can be rewritten to

$$\begin{aligned} x(k + 1) &= \bar{A}_d(k)x(k) + \bar{B}_d(k)u(k) + \bar{f}_1(k) + \bar{w}(k) \\ y(k) &= Cx(k) + F_f f_2(k) + v(k), \end{aligned} \quad (12)$$

where the matrices are given by

$$\bar{A}_d(k) = \Phi((k + 1)\Delta t, k\Delta t), \quad \bar{B}_d(k) = \int_{k\Delta t}^{(k+1)\Delta t} \Phi((k + 1)\Delta t, \tau)\bar{B}(\tau)d\tau. \quad (13)$$

Under the given assumptions, the Wiener integral  $\bar{w}(t) = \int_t^{t+\Delta t} \Phi(t + \Delta t, \tau)E_w dw_\tau$  is normally distributed with mean the zero vector and variance equal to

$$\Sigma(t) = \int_t^{t+\Delta t} \Phi(t + \Delta t, \tau)E_w E_w^T \Phi(t + \Delta t, \tau)^T d\tau. \quad (14)$$

By changing the matrix  $E_w$ , the variance of the Brownian motion can be adjusted accordingly. All these considerations follow from Davis [4].

## 4.2 Assumptions

Before the fault detection strategy is discussed, the assumptions the construction of the approach is based on are considered.

First, the method used is applied to equations of the form of Equation (8). Second, the disturbance vector  $w(k)$  and the noise vector  $v(k)$  are assumed to be white Gaussian random vectors. Third,  $w(k)$  and  $v(k)$  are assumed to be independent. The initial state  $x_0$  satisfies

- $E[x_0] = \bar{x}_0$
- $\text{Cov}[x_0] = \Sigma_0$
- $x_0$  is a Gaussian random vector.

The last assumption is that  $u(k)$  is deterministic. For instance, when  $u(k)$  is determined via a feedback loop, it depends on the estimate of the state vector. Given this estimate,  $u(k)$  can be calculated. If no additional noise is present in the actuator, the  $u(k)$  given to the system equals the (known) calculated  $u(k)$ . In this sense,  $u(k)$  can be viewed as deterministic.

### 4.3 A Kalman filter approach to fault detection

In this section, a Kalman filter is designed to perform fault detection under the assumptions of Section 4.2. The test statistics of Chapter 3 are not used immediately because the required conditions are not satisfied. If the output measurements  $y$  are used, the values of  $y$  at different times are not independent. The test statistics in Chapter 3 use independent measurements. As a consequence, the test statistics employed in that chapter cannot be used immediately. Additionally, the test statistics use stationary random variables. As the distribution of  $y$  is not stationary,  $y$  can not immediately be used.

These problems are resolved using a Kalman filter. The idea of using the Kalman filter is taken from Ding [5]. By applying a Kalman filter, new information is generated. Using this new information, a variable is generated that does satisfy the independence property. This variable is not yet stationary. However, as the covariance matrix is known, this variable can be made stationary. By combining the test statistics with the new variable, faults can be detected. After some notation has been introduced, the Kalman filter based residual generation and residual evaluation procedure is presented.

The first important variable with respect to the Kalman filter is the prediction of the next state and is denoted by  $\hat{x}(k+1|k) = E[x(k+1)|y(0), y(1), \dots, y(k), u(0), \dots, u(k)]$ . The estimated output is given by  $\hat{y}(k+1|k) = C\hat{x}(k+1|k) + Du(k+1)$ . The error between the estimate  $\hat{y}(k|k-1)$  and the actual output  $y(k)$  is denoted by  $e(k) = y(k) - \hat{y}(k|k-1)$ . The parameter  $n_e$  is the number of entries in  $e$ . Let  $l = n \cdot n_e$  and let  $D_i$  be the covariance matrix of  $e(i)$ .

The models used for fault detection using a Kalman filter resemble Equation (8). Using a Kalman filter on these equations, an estimate  $\hat{y}(k+1|k) = C\hat{x}(k+1|k) + Du(k+1)$  of  $y(k+1)$  can be obtained before  $y(k+1)$  is observed. After  $y(k+1)$  is observed,  $e(k+1) = y(k+1) - \hat{y}(k+1|k)$  can be generated. To use  $e(k+1)$  in combination with statistical properties of the Kalman filter, it is assumed that  $D_{k+1}$  is positive definite. It follows from Appendix A that the positive definite square root  $(D_i^{-1})^{\frac{1}{2}}$  of the positive definite matrix  $D_i$  is unique,  $\bar{X}(k) = \frac{1}{n \cdot n_e} \sum_{i=k}^{k+n-1} \sum_{j=1}^{n_e} ((D_i^{-1})^{\frac{1}{2}} e(i))_j \sim \mathcal{N}(0, \frac{1}{l})$  and  $S^2(k) = \sum_{i=k}^{k+n-1} e(i)^T D_i^{-1} e(i) \sim \chi_l^2$  in the nonfaulty situation. The quantities  $\bar{X}(k)$  and  $S^2(k)$  are equivalent to the test statistics  $Z$  and  $X_n^2$  introduced in Section 3.1 with measurements the entries of  $(D_i^{-1})^{\frac{1}{2}} e(i)$  ( $i \in \{k, k+1, \dots, k+n-1\}$ ). Hence, with respect to the entries of  $(D_i^{-1})^{\frac{1}{2}} e(i)$  ( $i \in \{k, k+1, \dots, k+n-1\}$ ), the test statistic  $\bar{X}(k)$  is designed to detect changes in the mean and  $S^2(k)$  is a test statistic designed to detect changes in the variance.

Using models resembling Equation (8), the test statistics  $\bar{X}(k)$  and  $S^2(k)$  can be used in combination with their statistical properties mentioned in the previous paragraph to test the following hypothesis

- $H_0$ : no fault is present in the system ( $f_i(s) = 0$  (for  $i \in (1, 2)$ ),  $A_f(s) = 0$  and  $B_f(s) = 0$  for  $s \in [0, t]$ ).
- $H_1$ : a fault is present in the system ( $f_i(s)$  (for either  $i = 1$  or  $i = 2$ ),  $A_f(s)$  or  $B_f(s)$  is nonzero for some  $s \in [0, t]$ ).

Using two sided tests, the null hypothesis is either accepted or rejected. A two-sided test was chosen over a one-sided test because what effect the faults in the system have on the mean and the variance of the test statistics was not known. To perform the hypothesis testing, samples were generated. The samples used for the hypothesis testing can be generated by using either a sliding window or fully separated batches. To explain what a

sliding window means, assume that  $k + n - 1$  measurements have been performed. After the  $(k + n - 1)$ th measurement,  $S^2(k)$  and  $\bar{X}(k)$  are used as test statistics. After one time step, the  $(k + n)$ th measurement has been acquired. After this measurement,  $S^2(k + 1)$  and  $\bar{X}(k + 1)$  can be used as test statistics. If fully separated batches are used,  $S^2(k + n)$  and  $\bar{X}(k + n)$  are used after  $S^2(k)$  and  $\bar{X}(k)$ . In Appendix D, a discussion about the choice for the sliding window or the fully separated batches approach is provided. In the rest of this paper, the fully separated batches were used due to their simplicity in calculating false alarm rates under the used assumptions.

## 5 Investigating complications Kalman filter based detection algorithm

To investigate (speed) complications of the algorithm given in Section 4.3, simulations of a DC motor were performed. To perform these simulations, the discretisations of Subsection 4.1.2 were used in combination with the dynamical equations in Subsection 4.1.1. When simulations are described, which discretisation strategy is employed is stated.

### 5.1 Testing the algorithm

Before discussing the (speed) complications with respect to the algorithm, results are shown that demonstrate that the algorithm works. For the simulations, the discretisation given by Equations (8) and (9) was used in combination with  $\Delta t = 0.001$ . Moreover, the parameters as described in Tables 1 and 2 were used.

TABLE 1: Values of the parameters for scenario 1.

Parameter	Value	Unit
$R$	0.5	Ohm
$L$	0.003	Henry
$J$	0.0167	kgm <sup>2</sup>
$k_m$	0.8	V/rad/sec
$D_v$	0.01	Nm/rad/sec
$T_l$	0	Nm

TABLE 2: Values of the parameters for scenario 2.

Parameter	Value	Unit
$R$	0.5	Ohm
$L$	1	Henry
$J$	1	kgm <sup>2</sup>
$k_m$	0.5	V/rad/sec
$D_v$	0.01	Nm/rad/sec
$T_l$	0	Nm

Furthermore,

$$w(k) \sim \mathcal{N}(0, A_1), v(k) \sim \mathcal{N}(0, A_2), x_0 \sim \mathcal{N}(0, A_3), \quad (15)$$

where  $0$  denotes the zero vector of appropriate dimensions and

$$C = [0 \ 1], A_1 = \begin{bmatrix} 120 & 0 \\ 0 & 120 \end{bmatrix}, A_2 = 0.1, A_3 = \begin{bmatrix} 0.01 & 0 \\ 0 & 0.01 \end{bmatrix}. \quad (16)$$

The fault occurs at 7.5 seconds and the used input (unless otherwise mentioned) is given by

$$u(t) = \begin{cases} 6t & \text{if } t < 0.1, \\ 6 & \text{otherwise.} \end{cases} \quad (17)$$

The time window in which the fault needs to be detected is 7.5 seconds and the level of confidence was taken to be 99.99%. Additionally, a sample consists of 50 measurements. Before presenting the results, some remarks are necessary. First,  $T_l$  was assumed to equal zero. This seems odd, but it was assumed that the load torque disturbance  $T_l$  is present in the second entry of the disturbance vector  $w(k)$ . Inspecting Equation (4), this is justified

as long as the inertia  $J$  is kept constant. Moreover, a high confidence level is necessary. If a 95% confidence level had been chosen, on average  $\frac{7.5}{0.00150} \cdot 0.05 = 7.5$  false alarms would have occurred in the 7.5 seconds in which no fault occurred. This is not desirable. Lastly, when a fault in the DC motor has critical consequences, the level of confidence should be lower in order to detect the critical fault more quickly. When a fault is less critical, a higher level of confidence can be used. This was discussed in Section 3.2.3 as well.

The results of the simulations are presented in Appendix C. Tables 3 and 4 summarise these results. If Table 3 or 4 indicates that a fault is reliably detectable using the algorithm of Section 4.3, the fault is almost always detected within 7.5 seconds by an alarm of  $\bar{X}(k)$  or  $S^2(k)$ . Moreover, the magnitude of the fault cannot be taken much smaller. If it is taken much smaller, the probability to detect the change with  $\bar{X}(k)$  or  $S^2(k)$  within 7.5 seconds decreases and the fault is not reliably detectable. Hence, the values in Tables 3 and 4 give an order of magnitude for the faults that can be detected reliably using the algorithm from Section 4.3.

TABLE 3: Results of the simulations of different faults when using the algorithm from Section 4.3 and adopting the parameters of scenario 1 (see Table 1). A fault is called (reliably) detectable if it has a high probability to be detected using the algorithm of Section 4.3.

Fault description	Changed to	Detectable
Change in resistance $R$	$R_{new} = 2.5R$	Yes
Change in inductance $L$	$L_{new} = 7.5L$	Yes
Change in friction $D_v$	$D = 3D_v$	Yes
Actuator fault: a higher input	$u = 6$ to $u = 6.08$	Yes
Actuator fault: a loss of effectiveness	$u = 6\sin(\pi t)$ to $u = 5.9\sin(\pi t)$	Yes
Additional disturbance in system	$f_1(k) \sim [\mathcal{N}(0, 10 \cdot 120), \mathcal{N}(0, 10 \cdot 120)]^T$	Yes
Additional disturbance in sensor	$f_2(k) \sim \mathcal{N}(0, 0.05)$	Yes
Sensor bias	$f_2(k) = 0.1$	Yes

TABLE 4: Results of the simulations of different faults when using the algorithm from Section 4.3 and adopting the parameters of scenario 2 (see Table 2). A fault is called (reliably) detectable if it has a high probability to be detected using the algorithm of Section 4.3.

Fault description	Changed to	Detectable
Change in resistance $R$	$R_{new} = 100R$	No
Change in inductance $L$	$L_{new} = 100L$	No
Change in friction $D_v$	$D = 50D_v$	Yes
Actuator fault: a higher input	$u = 6$ to $u = 11$	Yes
Actuator fault: a loss of effectiveness	$u = 6\sin(\pi t)$ to $u = 0$	No
Additional disturbance in system	$f_1(k) \sim [\mathcal{N}(0, 4 \cdot 120), \mathcal{N}(0, 4 \cdot 120)]^T$	Yes
Additional disturbance in sensor	$f_2(k) \sim \mathcal{N}(0, 0.05)$	Yes
Sensor bias	$f_2(k) = 0.5$	Yes

Table 3 shows that in principle, many faults can be detected. The system quickly achieves a steady state, so identifying shortcomings is simple. However, the tests indicate that many faults can be detected. This does not mean that the same faults can be detected in a

different situation. To see whether the ability to detect certain faults relies on the situation, Table 3 can be compared with Table 4. This comparison shows that the ability to detect a specific kind of fault depends on the situation. Therefore, the complications with respect to the algorithm depends on the situation. In addition, Table 4 shows that some large changes cannot always be reliably detected using the fault detection algorithm. It could be that the algorithm cannot detect these faults as the effect of the fault on the angular velocity is small. In this case, detecting the fault is difficult and the failure of detecting the fault is not because the algorithm is bad. To investigate whether the fault is difficult to detect using the algorithm or that the faults are hard to detect in general, simulations were performed. These simulations satisfied the same assumptions as the simulations used to generate table 2. The simulations graphed the actual angular velocity in the faulty case. In addition, they graphed the angular velocity as if no fault occurred. This angular velocity is simulated by using the equations in the nonfaulty case in combination with exactly the same disturbances and inputs as used in the faulty simulation. Graphs for a change in the resistance, a change in the inductance and a loss of effectiveness in the actuator can be found in Figures 14 up to and including 16 in Appendix E. In these simulations, the faults were not detected. These figures show that there is a considerable difference between the actual angular velocity and the angular velocity as if no fault occurred. As a consequence, it is expected that the algorithm is bad in detecting the indicated faults and another algorithm may detect the faults.

## 5.2 Complications when performing fault detection

In this section, some complications that might arise when performing fault detection are discussed. These complications range from using a certain number of measurements per sample to why certain faults cannot be detected using the designed algorithm.

### 5.2.1 Detecting a change in the variance using a test statistic for the mean

A simulation of the 'More stochastic disturbance in the system' fault of Table 4 yields the alarms given in Figure 21 in Appendix E. The assumptions under which Table 4 was generated, were used in this simulation as well.

Figure 21 in Appendix E shows that the test statistic  $\bar{X}(k)$  for the mean detects the increase in the variance of the process disturbance. We expected the test statistic  $S^2(k)$  for the variance to detect an increase in the variance of the disturbance in the system, but it did not. Nevertheless, Figure 21 is only one simulation, so this could have been a coincidence. To investigate whether it is a coincidence, the probability of detecting the fault within 7.5 seconds was estimated by performing 50 measurements. For  $\bar{X}(k)$ , the estimate is  $\frac{49}{50}$ . For  $S^2(k)$ , the estimate is  $\frac{6}{50}$ . Due to this big difference,  $\bar{X}(k)$  is preferred over  $S^2(k)$  considering the 'More stochastic disturbance in the system' fault of Table 4. This is not what we initially expected.

### 5.2.2 Adapting to the fault and a related problem with sensor bias faults

The statistics  $\bar{X}(k)$  and  $S^2(k)$  depend on the number of measurements per sample  $n$ . Increasing  $n$  yields more certainty and smaller confidence intervals. However, the system may correct the fault. If the system quickly corrects the fault, the effect of the fault on the residual signal is most likely very small as only some values of the residual signal are affected by the fault. Additionally, observers and Kalman filters react to faults. When a Kalman filter is applied, the estimate of the state is obtained by making a correction based

on the measurements. This occurs via the equation  $\hat{x}(k|k) = \hat{x}(k|k-1) + K(k)(y(k) - C\hat{x}(k|k-1) - Du(k))$ . Therefore, the Kalman filter might adapt to the fault. If the fault occurs for the first time, the Kalman filter is not adapted to the fault. At that moment, the behaviour of the residual signal may change due to the fault. Subsequently, the residual signal might adapt to the fault.

For both the system and Kalman filters adapting to the fault, by selecting too large an  $n$ , the effect of these small number of residual values indicating a fault is small due to the considerations discussed in Section 3.3. As a consequence, the fault may not be detected. In case of the Kalman based residual generator and a sensor fault, the residual signal  $e(i) = y(i) - \hat{y}(i|i-1)$  behaves as shown in Figure 7. The fault is only present for a short time after the occurrence of the fault. As the input is given by Equation (17) and the sensor can only have an influence on the system via the input,  $x(i)$  is not influenced by the fault in the sensor. As a consequence, the Kalman filter quickly adapts to the fault. When designing a fault detection algorithm, the designer needs to be cautious with such scenarios.

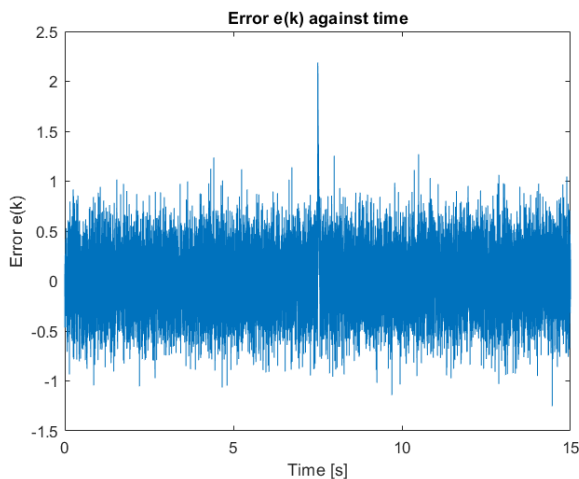


FIGURE 7: The error function when a sensor bias of 2 starting at 7.5 seconds occurs. For the simulation the assumptions used to obtain Table 4, were used.

### 5.2.3 Explaining the difficulty to detect a change in parameters

Table 4 shows that parameter changes were not detected reliably during the simulations. Observers do not detect multiplicative faults well [10], but stating this does not explain why they do not detect multiplicative faults well. For the algorithm from Section 4.3, equations are used to explain why multiplicative faults are hard to detect.

Assume a system with no faults behaves according to the following discrete equations

$$x(i+1) = Ax(i) + Bu(i) + E_w w(i), \quad y(i) = Cx(i) + v(i),$$

where  $w(i)$  and  $v(i)$  are independent Gaussian random vectors. Let  $e_x(i+1) = x(i+1) - \hat{x}(i+1|i)$ . Furthermore, assume that at moment  $k$ , a parameter changes and causes the matrices  $A$  and  $B$  to change to  $A + A_f$  and  $B + B_f$ , respectively. Define  $e_{x,0}(i+1) = x_0(i+1) - \hat{x}_0(i+1|i)$  as the part of  $e_x(i+1)$  that describes the part of  $e_x(i+1)$  that acts according to the nonfaulty dynamics. For a better description of the variable  $e_{x,0}(i+1)$ , see appendix B. If no fault occurs,  $e_x(i+1) = e_{x,0}(i+1)$ . It can be shown that  $e_x(i+1) = e_{x,0}(i+1) + e_f(i+1)$ . The part  $e_f(i+1)$  is given by the following recursive formula

$$e_f(i+1) = A(I - AK(i+1)C)e_f(i) + A_f x(i+1) + B_f u(i+1) \quad (18)$$

where  $K(i + 1)$  is the Kalman gain matrix. The initial conditions are given by

$$e_f(k) = A_f x(k) + B_f u(k). \quad (19)$$

For the derivation, see Appendix B. For ease of notation, let  $Y = A(I - AK(i + 1)C)$  and  $c(i) = A_f x(i) + B_f u(i)$ . Then it can easily be shown that

$$e_f(k + i) = \sum_{j=k}^{k+i} Y^{k+i-j} c(j). \quad (20)$$

Using Equation (20), the detectability of parameter changes is discussed. Consider the scenario where the parameters are given by Table 2 and Equations (15) to (17) apply. Furthermore, the fault occurs at 7.5 seconds. By applying the discretisation method described by Equations (8) and (9) on the nonfaulty DC motor equations in Equation (4), the matrices were obtained that were used in Equations (18) to (20). The time steps in the simulation were taken to be  $\Delta t = 0.001$ . The simulations showed that the gain matrix  $K(i + 1)$  achieved a steady state value before the 7.5 seconds passed. This steady state value, the discretised matrix of the  $A$  matrix given in Equation (4) and  $C = \begin{bmatrix} 0 & 1 \end{bmatrix}$  were used to calculate  $Y$  in Equation (20). For the described scenario

$$Y = \begin{bmatrix} 0.995 & -0.0139 \\ 0.0005 & 0.9658 \end{bmatrix}. \quad (21)$$

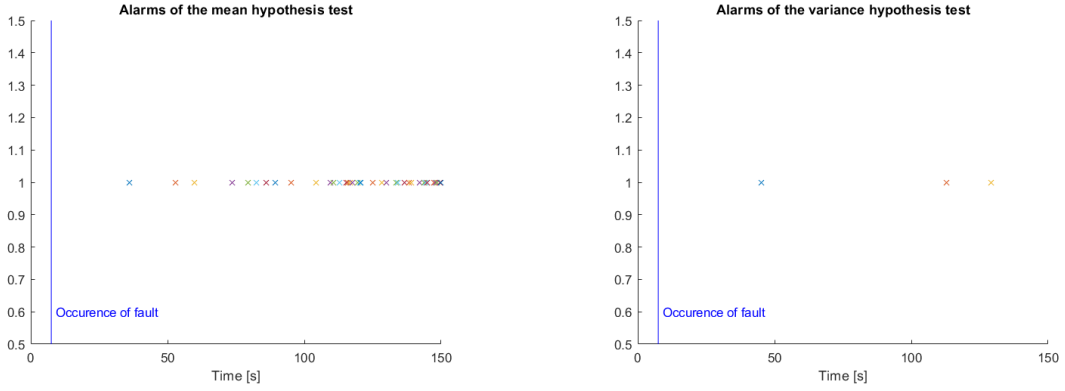
Equations (20) and (21) were used to examine the inability to detect the faults in the parameters. First, simulations were performed where the resistance value  $R$  changes to  $100R$  at  $t = 7.5$ . Inspecting Equation (4), the change in  $R$  results in the discrete fault matrix  $A_f = \Delta t \begin{bmatrix} \frac{100}{1} & 0 \\ 0 & 0 \end{bmatrix} = \begin{bmatrix} 0.1 & 0 \\ 0 & 0 \end{bmatrix}$ . The discrete fault matrix  $B_f = 0$  with  $0$  the zero matrix of appropriate dimensions. Using Equation (20) in combination with the previously determined matrices, yields

$$e_f(k + i) = \sum_{j=k}^{k+i} Y^{k+i-j} c(j) = \sum_{j=k}^{k+i} Y^{k+i-j} A_f x(j) = \sum_{j=k}^{k+i} Y^{k+i-j} \begin{bmatrix} 0.1I_j \\ 0 \end{bmatrix},$$

where  $I_j$  is the current at moment  $j$ . As only the angular velocity is measured, the fault detection algorithm only sees

$$C e_f(k + i) = \sum_{j=k}^{k+i} C Y^{k+i-j} \begin{bmatrix} 0.1I_j \\ 0 \end{bmatrix} = \sum_{j=k}^{k+i} \left( Y^{k+i-j} \right)_{21} \cdot 0.1I_j, \quad (22)$$

where  $\left( Y^{k+i-j} \right)_{21}$  is the element in position (2, 1) of the matrix  $Y^{k+i-j}$ . Simulating the faults yielded that the current  $I$  and  $\left( Y^{k+i-j} \right)_{21}$  are small. For results of the performed simulations, see Figures 18 and 19 in Appendix E. It can be seen that the terms in Equation (22) are small due to the small values of  $0.1I_j$  and the small values of  $Y^{k+i-j}$ . It is likely that the sum in Equation (22) is small due to not enough terms being summed. As a consequence, the change in the parameters is not seen in the residual vector. If more terms are summed, the sum may become larger and the fault can be detected later on. Simulations with the scenario used in Table 4 were done to investigate this. The only difference with the simulations used to obtain Table 4 is that instead of a 99.99% confidence level, a 99.9% confidence level was used. The results are shown in Figures 8 and 9.



(A) Alarms of the  $\bar{X}(k)$  test statistic.

(B) Alarms of the  $S^2(k)$  test statistic.

FIGURE 8: The alarms given during a simulation of a fault in the resistance going from  $R$  to  $100R$  for the situation used in Table 4. Instead of a 99.99% confidence level, a 99.9% confidence level was used.

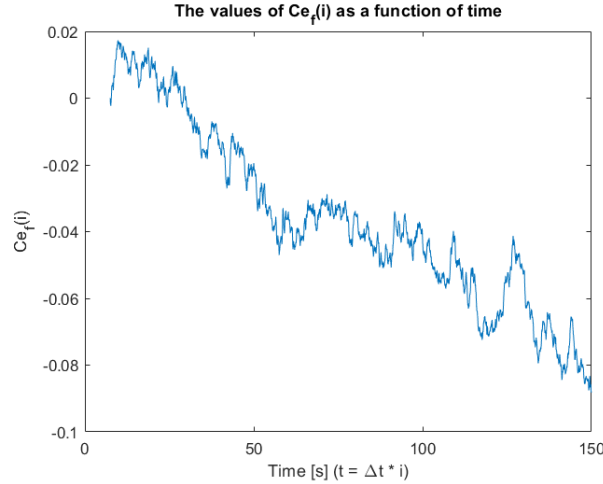


FIGURE 9: The  $Ce_f$  for a simulation of a fault in the resistance going from  $R$  to  $100R$  for the situation used in Table 4. Instead of a 99.99% confidence level, a 99.9% confidence level was used.

Figure 9 show that as time progresses, the sum in Equation (22) becomes larger. In addition, by comparing Figures 8 and 9, the relation between  $Ce_f$  and detecting faults is eminently clear. As expected, the larger the magnitude of  $Ce_f$ , the more alarms are given. As a consequence, to not wait longer than 7.5 seconds to detect the fault, a change in some properties might enlarge the sum and make the fault better detectable. When  $I_j$  is larger in magnitude for a lot of  $j$  values, the sum is enlarged and the change in the resistance is more likely to be detected. In a DC motor, if the voltage is increased, the current increases. Hence, by choosing a higher input voltage,  $I_j$  is higher and the fault in the resistance could be detected. Furthermore, for our case, the detection algorithm could improve if  $Y$  is adapted such that  $(Y^i)_{21}$  achieves a larger magnitude. As  $Y = A(I - AKC)$  with  $K$  being the steady-state Kalman gain,  $Y$  can be adapted by choosing a different  $K$ . Hence, choosing a suitable  $K$  can increase the performance of the algorithm. However, the properties of the Kalman filter might not apply if the matrix  $K$  is changed, so care must be taken.

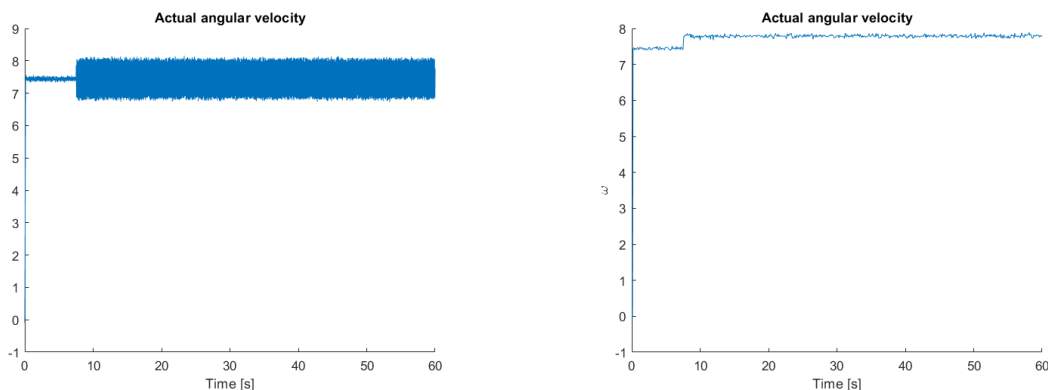
### 5.2.4 Influence of the sampling interval

When performing fault detection, it is possible to choose the sampling interval. The algorithm can be designed to obtain new measurements and calculate the Kalman filter estimate every 0.001 seconds or every 0.1 seconds. If the Kalman estimate is only calculated every 0.1 seconds, more uncertainty is present. As a consequence, the Kalman estimates of  $x$  at time  $t$  are more precise if every 0.001 seconds measurements are done and Kalman estimates are calculated.

However, this complicates the situation. Consider the scenario where measurements are done every  $\Delta t$  seconds and the batches are  $t_s$  seconds long. If a fixed average number of false alarms in a given time window is given, a certain confidence level is determined using the procedure explained in Section 3.3. For different values of  $\Delta t$ , the confidence level for these batches remain the same due to the fact that  $t_s$  remains the same. Depending on the number of measurements in the batch, the confidence bounds do change. Furthermore, different values of  $\Delta t$  result in different behaviours of  $e(i) = C(x(i) - \hat{x}(i|i-1))$  by the earlier considerations. As the used test statistics depend on  $e(i)$ , the behaviour of the test statistics is different in both situations. Combining this with the different bounds makes it hard to say something about the dependency on  $\Delta t$  of the power without resorting to simulations.

Consider the case that every 0.5 seconds a hypothesis test is done. Furthermore, the confidence interval is determined such that 1 false alarm occurs on average every 120 seconds. As 240 hypothesis test are done in 120 seconds, the confidence level equals  $\alpha = 1 - \frac{1}{240}$ . It is assumed that the parameters in Table 1 are taken. Furthermore, the fault occurs at 7.5 seconds. Moreover, the fault that occurs behaves as a sawtooth function of 10 Hertz and is added to the input. Figure 17 in Appendix E shows 10 periods of this function.

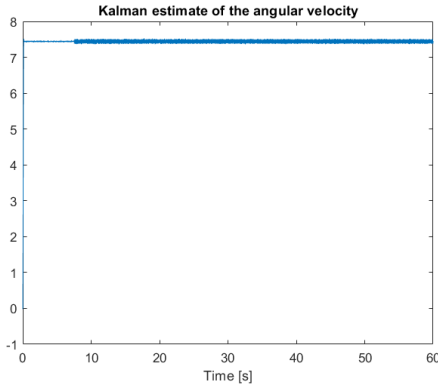
Simulations were done on this situation. For  $\Delta t = 0.001$ , the discretisation described by Equations (8) and (9) were utilized. Moreover, Equations (15) and (16) were used. For  $\Delta t = 0.1$ , Equations (11) up to and including (14) were used. In Equation (14),  $E_w = \sqrt{0.001}A^{\frac{1}{2}} = \sqrt{0.001} \begin{bmatrix} \sqrt{120} & 0 \\ 0 & \sqrt{120} \end{bmatrix}$  with  $A_1$  given in Equation (16). In our case,  $\bar{A} = A$  and  $\bar{B} = B$ . As a consequence,  $\Phi(t + \Delta t, \Delta t) = e^{A\Delta t}$ . In order to incorporate the extra sawtooth input, in the formula for  $\bar{f}_1(t)$ , let  $f_1(\tau)$  be the sawtooth function and  $E_f = B$ . The noise in the sensor  $v(k)$  is distributed according to Equation (15). For both simulations,  $u(t) = 6$ . The results are presented in Figures 10 up to and including 23.



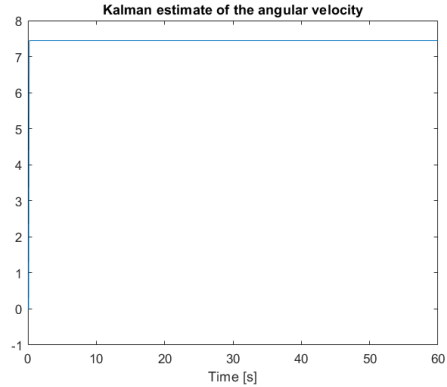
(A) Simulations with  $\Delta t = 0.001$ .

(B) Simulations with  $\Delta t = 0.1$ .

FIGURE 10: Plotting the angular velocity.



(A) Simulations with  $\Delta t = 0.001$ .



(B) Simulations with  $\Delta t = 0.1$ .

FIGURE 11: Kalman estimates belonging to Figure 10.

By comparing the figures in Figure 10, a difference is seen. The difference between the figures is due to aliasing. The system adapts to an input quite quickly. As after  $t = 7.5$  seconds  $u = 6 + f(t)$  with  $f(t)$  the sawtooth function, the system reacts to the sawtooth rapidly. This can be seen when zooming into Figure 10. The big variance change is not pure randomness. It is actually a sine of 10Hz with some additional noise components. If this sine is sampled with 10 Hz, a constant signal appears as in Figure 10b. Furthermore, by comparing Figures 10 and 11, the effect of the sampling interval on the residual signal  $e(i) = C(x(i) - \hat{x}(i|i-1))$ , is obvious. For  $\Delta t = 0.001$  a change in the variance occurs, while for  $\Delta t = 0.1$  the fault creates a change in the mean of the residual signal. As in the  $\Delta t = 0.001$  case, there is only an increase in the variance of  $e(i)$ , an increase in the variance occurs in  $(D_i^{-1})^{\frac{1}{2}}e(i)$  as  $(D_i^{-1})^{\frac{1}{2}}$  has already reached steady state when the fault occurred. In Section 3.4, it turned out that if only the variance changes, the  $X_n^2$  test statistic is preferred over the  $Z$  test statistic. As  $S^2(k)$  is basically equivalent to  $X_n^2$  and  $\bar{X}(k)$  is equivalent to  $Z$  (using the entries of  $(D_i^{-1})^{\frac{1}{2}}e(i)$  as measurements),  $S^2(k)$  should in general perform better than  $\bar{X}(k)$  when  $\Delta t = 0.001$ . Applying a similar story to the  $\Delta t = 0.1$  case, where only the mean of  $(D_i^{-1})^{\frac{1}{2}}e(i)$  is really changed, it is expected that  $\bar{X}(k)$  should perform better than  $S^2(k)$ . The alarms of the simulation depicted in Figures 10 and 11 are given in Figures 22 and 23 in Appendix E. Performing more simulations, yielded the same patterns as in Figures 22 and 23. The figures show that if  $\bar{X}(k)$  is used with an interval width of  $\Delta t = 0.1$ , the fault can be detected. On the other hand, when  $\Delta t = 0.001$  is used, the fault can not be detected. Similarly, when  $S^2(k)$  is used as test statistic, it is better to use  $\Delta t = 0.001$  instead of  $\Delta t = 0.1$ . Furthermore, it can be concluded, that in the  $\Delta t = 0.001$  case, in general, the power per batch is higher when using the  $S^2(k)$  test statistic. Similarly, in the  $\Delta t = 0.1$  case, generally the power per batch is higher when using the  $\bar{X}(k)$  test statistic.

In conclusion, if a specific test statistic is used (for instance  $\bar{X}(k)$ ) it might be sensible to try and change  $\Delta t$  as it might improve the power of the test statistic in a certain fault scenario. In our case, if initially  $\bar{X}(k)$  is taken and  $\Delta t = 0.001$ , it might be better to change  $\Delta t$  to 0.1.

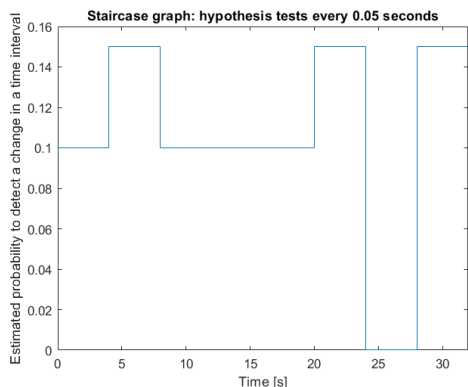
### 5.2.5 Increasing performance by suitable choice of $n$

In previous subsection, it is argued that given  $\Delta t$ , the test statistic can be changed to increase performance. Moreover, it is argued that given the test statistic,  $\Delta t$  can be

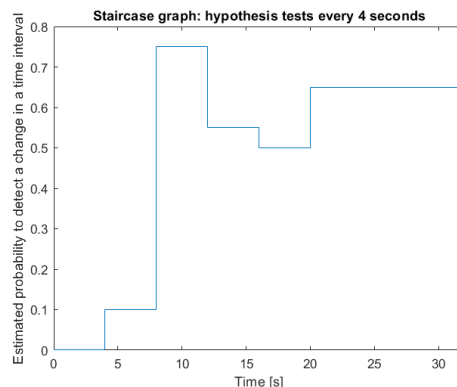
changed to increase performance. Guided by Sections 3.3 and 3.5, given a choice of  $\Delta t$ , an increase or a decrease in  $n$  might result in better performance.

The importance of suitably choosing  $n$  is investigated using the parameter fault as discussed in Subsection 5.2.3. This is illustrated using Figures 8 and 9. First of all, Figure 9 indicates a change of the mean over time. Furthermore, the variance does not seem to change a lot. Guided by comments in Section 3.4, the  $\bar{X}(k)$  test statistic most likely outperforms  $S^2(k)$ . Figure 8 confirms this.

Moreover, inferences regarding the number of measurements per sample can be made as well. In Section 3.3, it is mentioned that for a constant deviation from the normal value occurring only  $n_f$  consecutive measurements in only one specific batch, it is sensible to take the number of measurements per sample  $n$  equal to  $n_f$ . If this is not possible, one should take as many faulty measurements as possible. These considerations can be combined with Figure 9. This figure implies that in a particular simulation the faulty part  $Ce_f$  of the residual signal  $Ce_x = C(e_{x,0} + e_f)$  (see Subsection 5.2.3) has a mean of 0.01 for  $t$  between approximately 9 and 21 seconds. As a consequence, it might be more beneficial to increase the number of measurements per sample such that more faulty measurement for  $t$  between 9 and 21 are present in some sample. In order to test this hypothesis, 50 measurements per sample and 4000 measurements per sample are taken with  $\Delta t = 0.001$ . Simulations were done and the results are given in Figure 12. For the batches, a confidence level was used such that on average 2.4 false alarms occur every 120 seconds. Moreover, the values of Table 2 and Equations (15) up to and including (17) were used.



(A) Simulation results using 50 measurements per sample.



(B) Simulation results using 4000 measurements per sample.

FIGURE 12: 20 Simulations with new measurements every 0.001 seconds. The height of the graph indicates the estimated probability to give an alarm in the time interval  $[t, t + 3.999]$  with  $t \in \{0, 4, 8, 12, 16, 20, 24, 28\}$ .

In order to compare Figures 12a and 12b, one remark about Figure 12a is in place. The value for the interval  $[4, 7.999]$  is 0.15. If the interval  $[4, 7.5]$  is taken, the value is 0.15 as well. As the fault occurred at 7.5 seconds, it is implied that all given alarms in  $[4, 7.999]$  are false alarms. Taking this fact into account, a comparison can be made. It can be seen from Figure 12 that the estimated probability to detect a fault in the relevant region of  $t \geq 7.5$  is much larger when using 4000 measurements per sample instead of 50. Such a big difference is not a coincidence. As a consequence, we believe our intuition was indeed correct and increasing  $n$  yields better and faster detection in this scenario.

## 6 Discussion

In this paper, several assumptions were made in order to perform the analysis. For instance, in the dynamical case, it is assumed that the process disturbance and sensor noise are independent white Gaussian random vectors. Furthermore, the initial state is assumed to be a Gaussian random vector. Using these assumptions, properties of the Kalman filter could be applied. In real life, these assumptions may not apply. Moreover, real sensor noise has some form of memory. This is not incorporated into the models. Finally, in most systems some sort of feedback control is applied. In the analysis, no feedback is used. It is unknown if the complications treated in this paper transfer to the case where feedback is used. Combining the preceding arguments, the treated complications might not apply to real life systems. Additionally, the used system is a relatively simple system. As a consequence, the problems discussed in the paper might not transfer over to more complex systems. Finally, the static problem assumes normality of the samples for ease of analysis. This might be inapplicable to fault detection problems as well.

Even though the made assumptions may not apply to real life applications, the obtained results indicate what complications might arise in real situations. It is possible that the complications arise. As a consequence, the complications can be kept in mind when designing a fault detection algorithm. Furthermore, the obtained results using the assumptions can give us useful understandings and knowledge about these possible complications that might arise in real situations.

## 7 Conclusion

In this paper, several complications regarding fault detection are discussed. For some of the problems, reasons for their presence are provided. The complications were investigated using a static problem and a Kalman filter based fault detection algorithm.

Using the static problem, basic properties of the relation between hypothesis testing and the speed of detection were investigated. It turned out that in some scenarios there is a trade-off between the certainty to detect a fault and the probability that an incorrect fault alarm is given. In addition, taking the speed of detection into consideration, yielded another trade-off aspect. Additionally, some comments were made about adjustment of confidence levels in order to compare the performance under different number of measurements per sample. Furthermore, in case of a limited amount of faulty measurements, it turned out that taking more measurements per sample does not necessarily improve the probability to detect a fault. Moreover, some test statistics have been compared to each other. In different situations, other statistics may flourish. Finally, a connection between the probability to detect a fault and the time it takes to detect the fault, is made.

Using the static problem as basis, the dynamical case was treated. In the dynamical case, everything becomes much more complicated. Using a Kalman based fault detection algorithm, several complications were treated. For instance, it was argued that a fault detection algorithm may adapt to the fault and that the fault only affects the algorithm for a short amount of time. Using simulations, it was shown that this phenomenon occurred when applying a Kalman filter to a sensor bias fault in a DC motor. Additionally, the effect of a fault on the algorithm could be too small to detect the fault in a given time window. For a parameter fault in a DC motor, it is explained why the effect on the algorithm is too small. An increment of the Kalman gain is proposed in order to increase performance. Another approach that might work is to apply a parameter estimation method as this is more aimed at the parameters. These two approaches require further investigation. For

the parameter fault, in order to increase the fault detection performance, an adjustment of the number of measurements per sample is discussed. The general strategy employed in this discussion, can be employed to other faults as well. Finally, it is found that the sampling interval plays a role in the performance of a fault detection algorithm and should be taken into account.

All in all, the dynamical case is much more complicated than the static case. When designing a fault detection algorithm, the mentioned complications can possibly occur. As a consequence, one should always keep the complications in mind when creating a fault detection algorithm.

## 8 Recommendations future research

In this paper, additive process disturbance and additive sensor noise are discussed. Another type of disturbance and noise, is multiplicative disturbance and noise. Definitely in the process equations, multiplicative disturbance could be present. The complications arising due to multiplicative noise could be investigated. Moreover, in treating the dynamical case, the disturbance and noise vectors are assumed to be white Gaussian random vectors. If the distributions are not white and not Gaussian, the situation becomes more difficult. The new complications that arise in correlation with the extent of the existing complications can be investigated.

Additionally, the reasons behind the occurrence of some complications, are not discussed. In future research, more explanations may be given as well as more solutions to complications.

As indicated in the discussion (see Section 6), only relatively simple systems are treated. More complex systems have a more rich structure and therefore may yield more complications. In the future, this can be investigated. As indicated in the discussion, the effect of feedback is not discussed. According to Isermann [11], a control loop might compensate the fault. This resembles the behaviour for a sensor bias as discussed in Section 5.2.2. More anomalies might be present when considering feedback loops. It is interesting to investigate such anomalies.

Feedback loops are not the only aspect that is left out of consideration. In every dynamical system, modelling uncertainty is present. In case of much uncertainty, the performance of the fault detection algorithm relies on the robustness of the algorithm. If the algorithm is not robust, the performance of the algorithm is not that great. For further investigation, a linear system with model uncertainty in the system matrices can be designed. For investigating how robust fault detection algorithms can be created, we have found a book by Ding [5]. This book indicates that, for instance, Linear Matrix Inequality (LMI) techniques can be used to create a robust fault detection algorithm. After creating the robust fault detection scheme, complications regarding robust fault detection algorithms can be investigated.

In the conclusion (see Section 7), two approaches to solve the bad performance in detecting a change in the resistance in a DC motor are proposed. These methods require further investigation. Additionally, other observer methods can be investigated as well. These general observer methods may need to be made more sensitive to faults. The book by Ding [5] discusses a transfer function approach to make observers more sensitive to faults. This approach can be investigated and applied to the DC motor.

Another research topic is nonlinear systems. In this paper, the focus is on linear systems. Nonlinear systems are different from linear systems. It could be that new complications arise. Besides, due to the complexity of nonlinear systems, the solutions to the compli-

cations may become harder to find. The PhD thesis of Abid [1] discusses observer based fault detection approaches for nonlinear systems. Investigating some of these approaches and using them, complications of nonlinear systems can be researched. Additionally, it can be investigated how to deal with the complications.

Moreover, the paper only considers the scenario of one specific fault occurring and that the performance of a fault detection algorithm is examined only with respect to that fault. In systems, multiple faults may occur. In this sense, the performance of the fault detection algorithm depends on whether it can detect all possible faults that can occur as well. Designing an algorithm that can detect all possible faults in a system most likely yields more complications. Investigating such complications can perhaps be done using a Banks of Observers scheme [8].

Lastly, in the treatment of the dynamical case, residuals that were used are scalar valued. Vector valued residuals exist as well. For instance, under our assumptions, the Hotelling  $T^2$  distribution could perhaps be used in combination with a vector valued residual. Using this distribution, vector valued and scalar valued test statistics can be compared in terms of their fault detection performance.

## References

- [1] Muhammad Abid. *Fault detection in nonlinear systems: An observer-based approach*. PhD thesis, Universitat Duisburg-Essen, 2010.
- [2] Halim Alwi and Christopher Edwards. Fault detection and fault-tolerant control of a civil aircraft using a sliding-mode-based scheme. *IEEE Transactions on Control Systems Technology*, 16(3):499–510, 2008.
- [3] Daniele Brambilla, Luca M Capisani, Antonella Ferrara, and Pierluigi Pisu. Actuators and sensors fault detection for robot manipulators via second order sliding mode observers. In *2008 International Workshop on Variable Structure Systems*, pages 61–66. IEEE, 2008.
- [4] Mark H. A. Davis. *Linear estimation and stochastic control*. Chapman and Hall, 1977.
- [5] Steven X Ding. *Model-based fault diagnosis techniques: design schemes, algorithms, and tools*. Springer Science & Business Media, 2008.
- [6] Chuong Do. Stanford University Lecture Notes: More on Multivariate Gaussians. [http://cs229.stanford.edu/section/more\\_on\\_gaussians.pdf](http://cs229.stanford.edu/section/more_on_gaussians.pdf), May 2019.
- [7] Ulrich Faigle, Walter Kern, and Georg Still. *Algorithmic principles of mathematical programming*, volume 24. Springer Science & Business Media, 2013.
- [8] Paul M Frank. Analytical and qualitative model-based fault diagnosis—a survey and some new results. *European Journal of control*, 2(1):6–28, 1996.
- [9] Rolf Isermann. Process fault detection based on modeling and estimation methods - a survey. *automatica*, 20(4):387–404, 1984.
- [10] Rolf Isermann. Model-based fault-detection and diagnosis—status and applications. *Annual Reviews in control*, 29(1):71–85, 2005.
- [11] Rolf Isermann. *Fault-diagnosis systems: an introduction from fault detection to fault tolerance*. Springer Science & Business Media, 2006.

- [12] Charles R Johnson, Kazuyoshi Okubo, and Robert Reams. Uniqueness of matrix square roots and an application. *Linear Algebra and its applications*, 323(1-3):51–60, 2001.
- [13] Ramu Krishnan. *Electric motor drives: modeling, analysis, and control*, volume 626. Prentice Hall New Jersey, 2001.
- [14] Wei Li, Minjun Peng, and Qingzhong Wang. Improved pca method for sensor fault detection and isolation in a nuclear power plant. *Nuclear Engineering and Technology*, 51(1):146–154, 2019.
- [15] Jan M Maciejowski and Colin N Jones. Mpc fault-tolerant flight control case study: Flight 1862. *IFAC Proceedings Volumes*, 36(5):119–124, 2003.
- [16] D. Meijer and K. Poortema. Lecture Notes University Of Twente: Mathematical statistics with applications.
- [17] Dubravko Miljković. Fault detection methods: A literature survey. In *2011 Proceedings of the 34th international convention MIPRO*, pages 750–755. IEEE, 2011.
- [18] Olaf Moseler and Rolf Isermann. Application of model-based fault detection to a brushless dc motor. *IEEE Transactions on industrial electronics*, 47(5):1015–1020, 2000.
- [19] Riccardo Muradore and Paolo Fiorini. A pls-based statistical approach for fault detection and isolation of robotic manipulators. *IEEE Transactions on Industrial Electronics*, 59(8):3167–3175, 2011.
- [20] Maria Isabel Ribeiro. Kalman and extended kalman filters: Concept, derivation and properties. *Institute for Systems and Robotics*, 2004.
- [21] Ali Zolghadri, Jérôme Cieslak, Denis Efimov, David Henry, Philippe Goupil, Rémy Dayre, Anca Gheorghe, and Hervé Leberre. Signal and model-based fault detection for aircraft systems. *IFAC-PapersOnLine*, 48(21):1096–1101, 2015.

## A Proof distribution $\bar{X}(k)$ and $S^2(k)$

Before discussing the proof, some remarks are in place. As the proof uses theory about positive (semi) definite matrices, we refer the reader to Kern [7] for the utilized properties. Furthermore, the model that is treated in this Appendix is described by

$$x(k+1) = A_k x(k) + B_k u(k) + G_k w(k), \quad y(k) = C_k x(k) + D_k u(k) + v(k)$$

Moreover, the assumptions of Section 4.2 apply. That being said, the proof is now discussed.

By the assumptions and by definition of a Gaussian vector, it is easily verified that  $(x(k), y_0, y_1, \dots, y_{k-1} | u_0, u_1, \dots, u_{k-1})$  follows a Gaussian distribution. It is known that if  $(x_a, x_b)$  follows a Gaussian distribution,  $(x_a | x_b)$  follows a Gaussian distribution as well [6]. From this, it follows that  $(x(k) | y_0, y_1, \dots, y_{k-1}, u_0, \dots, u_{k-1})$  follows a Gaussian distribution. From the properties of the Kalman filter, we know that the estimate of the Kalman filter satisfies  $\hat{x}(k+1|k) = E[x(k+1) | y_0, y_1, \dots, y(k), u_0, \dots, u(k)]$ . Furthermore, under our assumptions the Kalman filter puts out  $\Sigma_{k+1|k} = \text{Cov}(x(k+1) - \hat{x}(k+1|k) | y_0, y_1, \dots, y(k), u_0, \dots, u(k))$ . Using the preceding properties, we obtain

$$x(k+1) - \hat{x}(k+1|k) | y_0, y_1, \dots, y(k), u_0, \dots, u(k) \sim \mathcal{N}(0, \Sigma_{k+1|k})$$

It is given that  $y(k) = C_k x(k) + D_k u(k) + v(k)$ , where  $v(k)$  has covariance matrix  $R_k$ . Furthermore, let  $\hat{y}(k|k-1) = C_k \hat{x}(k|k-1) + D_k u(k)$ . If  $X \sim \mathcal{N}(\mu, \Sigma)$  and  $b$  a deterministic vector,  $AX + b \sim \mathcal{N}(A\mu + b, A\Sigma A^T)$ . From Do [6], it is known that the sum of independent Gaussians  $X \sim \mathcal{N}(\mu_1, \Sigma_1)$  and  $Y \sim \mathcal{N}(\mu_2, \Sigma_2)$  satisfies  $X + Y \sim \mathcal{N}(\mu_1 + \mu_2, \Sigma_1 + \Sigma_2)$ . Using these properties, the following relationship is found

$$e(k) = y(k) - \hat{y}(k|k-1) \sim \mathcal{N}(0, C_k \Sigma_{k|k-1} C_k^T + R_k) = \mathcal{N}(0, D_k) \quad (23)$$

Before continuing the proof part that deals with  $e(k)$ , some properties of square roots of matrices need to be addressed. A square root of a matrix  $X$  is a matrix  $A$  such that  $A \cdot A = X$ . For the proof, it suffices to concentrate on symmetric positive definite matrices. Assume  $Y$  is a (symmetric) positive definite matrix. As  $Y$  is a (symmetric) positive definite matrix, there exists an invertible matrix  $Q$  such that  $D = QDQ^T$  where  $D$  is a diagonal matrix and  $QQ^T = I$  (with  $I$  the identity matrix). As  $Y$  is positive definite,  $D$  must have strictly positive entries on the diagonal. Therefore, the inverse of  $D$  exists and equals  $D^{-1} = \text{Diag}(\frac{1}{D_{11}}, \frac{1}{D_{22}}, \dots, \frac{1}{D_{nn}})$ . Using this information, a square root of  $Y^{-1}$  is found. The matrix  $Y^{-1}$  exists and is positive definite as  $Y$  is assumed to be positive definite. Let  $(Y^{-1})^{\frac{1}{2}} = Q(D^{-1})^{\frac{1}{2}}Q^T$  where  $(D^{-1})^{\frac{1}{2}} = \text{Diag}(\frac{1}{D_{11}}^{\frac{1}{2}}, \frac{1}{D_{22}}^{\frac{1}{2}}, \dots, \frac{1}{D_{nn}}^{\frac{1}{2}})$ . Furthermore, let  $D^{\frac{1}{2}} = \text{Diag}(D_{11}^{\frac{1}{2}}, D_{22}^{\frac{1}{2}}, \dots, D_{nn}^{\frac{1}{2}})$ . It can easily be verified that  $D^{\frac{1}{2}}$  and  $(D^{-1})^{\frac{1}{2}}$  are square roots of  $D$  and  $D^{-1}$ , respectively. Using  $QQ^T = Q^TQ = I$ , the given formulas for the square roots and the formulas for the inverse matrices,

$$(Y^{-1})^{\frac{1}{2}} Y = Q(D^{-1})^{\frac{1}{2}} Q^T Q D Q^T = Q(D^{-1})^{\frac{1}{2}} D Q^T = Q D^{\frac{1}{2}} Q^T$$

Using this, yields

$$(Y^{-1})^{\frac{1}{2}} Y (Y^{-1})^{\frac{1}{2}} = Q D^{\frac{1}{2}} Q^T (Y^{-1})^{\frac{1}{2}} = Q D^{\frac{1}{2}} Q^T Q (D^{-1})^{\frac{1}{2}} = Q D^{\frac{1}{2}} (D^{-1})^{\frac{1}{2}} = Q Q^T \quad (24)$$

$$= I$$

Furthermore, it is known that  $(Y^{-1})^{\frac{1}{2}} = Q(D^{-1})^{\frac{1}{2}}Q^T$  is positive definite as  $(D^{-1})^{\frac{1}{2}}$  is a diagonal matrix with positive entries on the diagonal and  $Q(Y^{-1})^{\frac{1}{2}}Q^T = (D^{-1})^{\frac{1}{2}}$ . As the positive definite square root of a positive definite matrix is unique [12],  $(Y^{-1})^{\frac{1}{2}} = Q(D^{-1})^{\frac{1}{2}}Q^T$  is the unique positive definite square root of  $Y^{-1}$  and  $(Y^{-1})^{\frac{1}{2}}Y(Y^{-1})^{\frac{1}{2}} = I$ . This result is utilized in the remainder of the proof. First, it is assumed that  $D_k = C_k \Sigma_{k|k-1} C_k^T + R_k$  is invertible. As covariance matrices are positive semi-definite and positive definite matrices are the invertible positive semi-definite matrices, this is equiv-

alent to  $D_k$  being positive definite. Using elementary properties of the positive definite covariance matrix  $D_k$  and the unique positive definite square root  $(D_k^{-1})^{\frac{1}{2}}$ , we obtain  $\text{Cov}((D_k^{-1})^{\frac{1}{2}} e(k)) = \text{Cov}((D_k^{-1})^{\frac{1}{2}} e(k), (D_k^{-1})^{\frac{1}{2}} e(k)) = (D_k^{-1})^{\frac{1}{2}} \text{Cov}(e(k), (e(k)) (D_k^{-1})^{\frac{1}{2}} = (D_k^{-1})^{\frac{1}{2}} D_k (D_k^{-1})^{\frac{1}{2}}$ . Using Equation (24) yields

$$\text{Cov}((D_k^{-1})^{\frac{1}{2}} e(k)) = I \quad (25)$$

From Ribeiro [20], it is known that  $e(k)$  is white. In other words,  $e(k)$  has a mean of zero and there is no correlation between  $e(i)$  and  $e(j)$  for  $i \neq j$ . Hence,  $\text{Cov}(e(i), e(j)) = 0$  for  $i \neq j$ . This yields

$$\text{Cov}((D_i^{-1})^{\frac{1}{2}} e(i), (D_j^{-1})^{\frac{1}{2}} e(j)) = (D_i^{-1})^{\frac{1}{2}} \text{Cov}(e(i), (e(j)) (D_j^{-1})^{\frac{1}{2}} = 0 \quad (26)$$

Let  $W = [X \ Y]^T$ . Calculating the covariance of  $W$  yields

$$\text{Cov}(W) = \begin{bmatrix} \text{Cov}(X) & \text{Cov}(X, Y) \\ \text{Cov}(Y, X) & \text{Cov}(Y) \end{bmatrix}$$

Letting  $X = (D_i^{-1})^{\frac{1}{2}} e(i)$  and  $Y = (D_j^{-1})^{\frac{1}{2}} e(j)$  ( $i \neq j$ ) and applying Equations (25) and (26) yields

$$\text{Cov}([(D_i^{-1})^{\frac{1}{2}} e(i)], (D_j^{-1})^{\frac{1}{2}} e(j)]^T) = \begin{bmatrix} \text{Cov}((D_i^{-1})^{\frac{1}{2}} e(i)) & 0 \\ 0 & \text{Cov}((D_j^{-1})^{\frac{1}{2}} e(j)) \end{bmatrix} = I \quad (27)$$

where  $I$  is the identity matrix of appropriate dimensions.

As  $e(i)$  and  $e(j)$  are Gaussian (see Equation (23)), so are  $(D_i^{-1})^{\frac{1}{2}} e(i)$  and  $(D_j^{-1})^{\frac{1}{2}} e(j)$ . It is known that the coordinates of a Gaussian vector  $X$  are independent if and only if the covariance matrix  $\text{Cov}(X)$  is diagonal. As a consequence, by Equation (27), all the entries of both  $(D_i^{-1})^{\frac{1}{2}} e(i)$  and  $(D_j^{-1})^{\frac{1}{2}} e(j)$  are independent with each other. In addition, as  $(D_i^{-1})^{\frac{1}{2}} e(i)$  is a Gaussian distribution with  $\text{Cov}((D_i^{-1})^{\frac{1}{2}} e(i)) = I$  and mean equal to the zero vector, every entry of  $(D_i^{-1})^{\frac{1}{2}} e(i)$  is a standard normal random variable. Recall that a  $\chi_f^2$  with  $f$  degrees of freedom is given by  $\sum_{k=1}^f Z_k^2$  where  $Z_k$  ( $k \in (1, 2, 3, \dots, f)$ ) are independent standard Normal random variables. As the entries of  $(D_i^{-1})^{\frac{1}{2}} e(i)$  are standard Normal random variables that are independent with all other entries of  $(D_i^{-1})^{\frac{1}{2}} e(i)$  and all entries of  $(D_j^{-1})^{\frac{1}{2}} e(j)$  for  $i \neq j$ , any sum of the squared entries is  $\chi^2$  distributed. As  $\left( (D_i^{-1})^{\frac{1}{2}} e(i) \right)^T (D_i^{-1})^{\frac{1}{2}} e(i) = e(i)^T ((D_i^{-1})^{\frac{1}{2}})^T (D_i^{-1})^{\frac{1}{2}} e(i) = e(i)^T D_i^{-1} e(i)$  is equal to the sum of the squares of the entries of  $(D_i^{-1})^{\frac{1}{2}} e(i)$ , it follows that  $\sum_{i=k}^{k+n-1} e(i)^T D_i^{-1} e(i)$  is a sum of the squares of the entries of  $(D_i^{-1})^{\frac{1}{2}} e(i)$  for  $i = k$  up to and including  $i = k+n$ . As all these entries are independent standard normal random variables, it follows that  $\sum_{i=k}^{k+n-1} e(i)^T D_i^{-1} e(i)$  follows a  $\chi_l^2$  distribution with  $l = n \cdot n_e$  the number of terms in the sum.

Moreover, as the entries of  $(D_i^{-1})^{\frac{1}{2}} e(i)$  are standard Normal random variables that are independent with all other entries of  $(D_i^{-1})^{\frac{1}{2}} e(i)$  and all entries of  $(D_j^{-1})^{\frac{1}{2}} e(j)$  for  $i \neq j$ ,  $\bar{X}(k) = \frac{1}{l} \sum_{i=k}^{k+n-1} \sum_{j=1}^{n_e} ((D_i^{-1})^{\frac{1}{2}} e(i))_j \sim \mathcal{N}(0, \frac{1}{l})$ .

## B Proof of Equations (18) and (19)

Assume a system with no faults behaves according to the following discrete equations

$$x(i+1) = Ax(i) + Bu(i) + E_w w(i), \quad y(i) = Cx(i) + v(i)$$

where  $w(i)$  and  $v(i)$  are random vectors. Furthermore, assume that at moment  $k$  a parameter changes and causes the matrices  $A$  and  $B$  to change to  $A + A_f$  and  $B + B_f$ , respectively. Using the discrete dynamics of the plant, it is obtained that

$$x(k+1) = Ax(k) + Bu(k) + E_w w(k) + A_f x(k) + B_f u(k) = x_0(k+1) + \bar{f}_k \quad (28)$$

Here  $x_0(k+1)$  indicates the value of  $x(k+1)$  given  $u(k)$  and no fault occurred. Assume  $x(i) = x_0(i) + \bar{f}_{i-1}$ . Using this assumption and the discrete dynamics of the plant,

$$\begin{aligned} x(i+1) &= Ax(i) + Bu(i) + E_w w(i) + A_f x(i) + B_f u(i) \\ &= Ax_0(i) + Bu(i) + E_w w(i) + A_f x(i) + B_f u(i) + A \bar{f}_{i-1} \\ &= x_0(i+1) + \bar{f}_i \end{aligned} \quad (29)$$

Combining the recursions in Equation (28) and (29), the following formula for the  $\bar{f}_i$  recursion can be obtained

$$\begin{aligned} \bar{f}_{i+1} &= A_f x(i+1) + B_f u(i+1) + A \bar{f}_i \\ \bar{f}_k &= A_f x(k) + B_f u(k) \end{aligned} \quad (30)$$

with  $\bar{f}_k$  the initial condition. Equation (30) can be used to write out the dynamics of the Kalman estimates. Doing so, we obtain

$$\begin{aligned} \hat{x}(k+1|k+1) &= \hat{x}(k+1|k) + K(k+1)(y(k+1) - C\hat{x}(k+1|k)) \\ &= \hat{x}(k+1|k) + K(k+1)(C(x_0(k+1) + \bar{f}_k) - C\hat{x}(k+1|k)) \\ &= \hat{x}_0(k+1|k+1) + K(k+1)C\bar{f}_k \end{aligned} \quad (31)$$

where  $\hat{x}_0(k+1|k+1)$  is the Kalman estimate  $\hat{x}(k+1|k+1)$  if no fault would have occurred. Similarly, using Equation (31), we obtain

$$\begin{aligned} \hat{x}(k+2|k+1) &= A\hat{x}(k+1|k+1) + Bu(k+1) \\ &= A\hat{x}_0(k+1|k+1) + Bu(k+1) + AK(k+1)C\bar{f}_k \\ &= \hat{x}_0(k+2|k+1) + f(k+1) \end{aligned}$$

with  $f_{k+1} = AK(k+1)C\bar{f}_k$  and  $\hat{x}_0(k+2|k+1) = A\hat{x}_0(k+1|k+1) + Bu(k)$  the Kalman estimate  $\hat{x}(k+2|k+1)$  given that no fault in the dynamics would have occurred. It could be that due to the fault the deterministic input  $u$  is changed. However, as it is deterministic this does not matter. Given that this new input is chosen, the Kalman estimates are calculated. In this sense,  $\hat{x}_0(k+2|k+1)$  and  $\hat{x}_0(k+1|k+1)$  are the Kalman estimates according to the non faulty dynamics. In other words, they are the Kalman estimates if the input can be adapted due to the fault, but the process is not adapted by the fault. Assume that it is given that  $\hat{x}(i+1|i) = \hat{x}_0(i+1|i) + f_i$  with  $\hat{x}_0(i+1|i)$  defined as earlier. Then following the same procedure, we obtain

$$\begin{aligned} \hat{x}(i+1|i+1) &= \hat{x}(i+1|i) + K(i+1)(y(i+1) - C\hat{x}(i+1|i)) \\ &= \hat{x}_0(i+1|i) + f_i \\ &\quad + K(i+1)(C(x_0(i+1) + \bar{f}_i) - C\hat{x}_0(i+1|i) - Cf_i) \\ &= \hat{x}_0(i+1|i+1) + K(i+1)C(\bar{f}_i - f_i) + f_i \end{aligned}$$

Using this, we obtain

$$\begin{aligned} \hat{x}(i+2|i+1) &= A\hat{x}(i+1|i+1) + Bu(i+1) \\ &= A\hat{x}_0(i+1|i+1) + Bu(i+1) + AK(i+1)C(\bar{f}_i - f_i) + Af_i \\ &= \hat{x}_0(i+2|i+1) + f(i+1) \end{aligned}$$

with  $f(i+1) = AK(i+1)C(\bar{f}_i - f_i) + Af_i$ . Define  $e_x(i) = x(i) - \hat{x}(i|i-1)$ . Using  $\hat{x}(i+1|i) = \hat{x}_0(i+1|i) + f_i$  and  $x(i+1) = x_0(i+1) + \bar{f}_i$ , it is obtained that  $e_x(i+1) = x_0(i+1) - \hat{x}_0(i+1|i) + \bar{f}_i - f_i = e_0(i+1) + e_f(i)$  where  $e_0(i+1)$  is the error if no fault

would have occurred (besides possible reconfiguration of the  $u$ ). The recursive formulas for  $f_i$  and  $\bar{f}_i$  are given by

$$\begin{aligned} f_{i+1} &= AK(i+1)C(\bar{f}_i - f_i) + Af_i \\ \bar{f}_{i+1} &= A_f x(i+1) + B_f u(i+1) + A\bar{f}_i \end{aligned}$$

with initializations

$$\begin{aligned} f_k &= 0 \\ \bar{f}_k &= A_f x(k) + B_f u(k) \end{aligned}$$

The initial condition for  $f_k$  is chosen such that  $f_{k+1} = AK(k+1)C\bar{f}_k$ . From these considerations, it can be inferred that

$$\begin{aligned} e_f(i+1) &= \bar{f}_{i+1} - f_{i+1} \\ &= A_f x(i+1) + B_f u(i+1) + A\bar{f}_i - (AK(i+1)C(\bar{f}_i - f_i) + Af_i) \\ &= A(I - AK(i+1)C)e_f(i) + A_f x(i+1) + B_f u(i+1) \end{aligned}$$

Using the initial conditions  $\bar{f}_k$  and  $f_k$ , the initial condition is given by

$$e_f(k) = \bar{f}_k - f_k = A_f x_k + B_f u_k$$

where we have to keep in mind that at moment  $k$  a fault occurred. In case of the assumptions in Section 4.2,  $e_0(i)$  is still a white Gaussian random vector as it is based on a deterministic input  $u$  and does not incorporate the faulty components. Hence, the distribution of this quantity is still the same as when no fault occurs. The part  $e_f(i)$  gives the faulty part in the residual generator and can be used for analysis.

## C Results simulations for different faults

TABLE 5: A description of the different fault types and assigning them a number

Fault type number	Description fault
1	Increase in resistance R
2	Increase in inductance L
3	Increase in friction $D_v$
4	Actuator fault: a higher input
5	Actuator fault: a loss of effectiveness
6	More stochastic disturbance in system
7	More stochastic disturbance in sensor
8	Sensor bias

TABLE 6: Defining different faults in terms of the dynamical system

Fault type number	Fault behaviour
1	$R$ changes to $R_{new}$
2	$L$ changes to $L_{new}$
3	$D_v$ changes to $D_{new}$
4	$u$ jumps from $u = 6$ to $u = u_{new}$
5	$u$ jumps from $6 \sin \pi t$ to $s \sin \pi t$ .
6	$f_1(k)$ in Equation (8) becomes $[\mathcal{N}(0, 120s), \mathcal{N}(0, 120s)]^T$ distributed ( $s \in \mathcal{R}$ )
7	$f_2(k)$ in Equation (8) becomes $\mathcal{N}(0, s)$ distributed ( $s \in \mathcal{R}$ )
8	$f_2(k) = s$ ( $s \in \mathcal{R}$ )

TABLE 7: The magnitude of the treated faults for the situation as described in Table 1. Furthermore, if  $R_{new} = 2.25R$ , 6 out of 18 simulations yielded a detection within 7.5 seconds by an alarm of  $\bar{X}(k)$  or  $S^2(k)$ . This quantity estimates the probability to detect the fault within 7.5 seconds. The description of the treated faults is in Table 6.

Fault type number	Treated faults	Estimate probability of detection
1	$R_{new} \in [1.5R, 2.25R, 2.5R]$	$[\frac{2}{18}, \frac{6}{18}, \frac{18}{18}]$
2	$L_{new} \in [3L, 5L, 7L, 7.5L]$	$[\frac{3}{18}, \frac{9}{18}, \frac{14}{18}, \frac{24}{24}]$
3	$D_{new} \in [2D_v, 2.5D_v, 3D_v]$	$[\frac{9}{18}, \frac{27}{30}, \frac{30}{30}]$
4	$u_{new} \in [6.02, 6.04, 6.08]$	$[\frac{2}{18}, \frac{6}{18}, \frac{24}{24}]$
5	$s \in [5.9, 5.96]$	$[\frac{18}{18}, \frac{5}{18}]$
6	$s \in [3.5, 5, 7, 10]$	$[\frac{4}{18}, \frac{11}{24}, \frac{18}{24}, \frac{18}{18}]$
7	$s \in [0.02, 0.05]$	$[\frac{4}{18}, \frac{18}{18}]$
8	$s \in [0.05, 0.08, 0.1]$	$[\frac{6}{18}, \frac{16}{18}, \frac{18}{18}]$

TABLE 8: The magnitude of the treated faults for the situation as described in Table 2. Furthermore, if  $R_{new} = 100R$ , 0 out of 12 simulations yielded a detection within 7.5 seconds by an alarm of  $\bar{X}(k)$  or  $S^2(k)$ . This quantity estimates the probability to detect the fault within 7.5 seconds. The description of the treated faults is in Table 6.

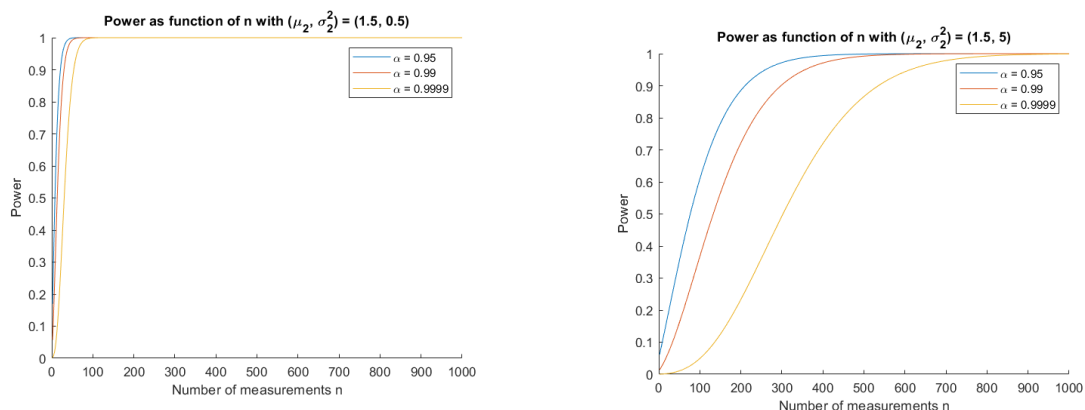
Fault type number	Treated faults	Estimate probability of detection
1	$R_{new} \in [100R]$	$[\frac{0}{12}]$
2	$L_{new} \in [100L]$	$[\frac{0}{12}]$
3	$D_{new} \in [30D_v, 40D_v, 50D_v]$	$[\frac{12}{18}, \frac{27}{30}, \frac{30}{30}]$
4	$u_{new} \in [8.2, 10, 11]$	$[\frac{5}{18}, \frac{17}{18}, \frac{18}{18}]$
5	$s \in [5, 2, 0]$	$[\frac{0}{18}, \frac{0}{18}, \frac{1}{18}]$
6	$s \in [1.5, 2, 3, 3.5, 4]$	$[\frac{8}{24}, \frac{18}{24}, \frac{34}{42}, \frac{23}{24}, \frac{24}{24}]$
7	$s \in [0.02, 0.05]$	$[\frac{6}{18}, \frac{18}{18}]$
8	$s \in [0.2, 0.3, 0.4, 0.5]$	$[\frac{0}{18}, \frac{7}{18}, \frac{12}{18}, \frac{18}{18}]$

## D Discussion sliding window and fully separated batch approach

The sliding window has an advantage over the method that uses fully separated batches. Assume we have 100 measurements and we use hypothesis testing with batches containing 10 measurements. Assume that a fault occurs at measurement 37. The fault is present for all later measurements as well. Furthermore, assume that the fault can be detected when 5 out of 10 measurements in a batch are faulty measurements. Using the method that uses fully separated batches, the batch containing measurements 41 up to and including 50 is the first batch to detect the fault. Using a sliding window, the batch containing measurements 33 up to and including 42 is the first batch that detects the fault. In this way, sliding windows could detect faults earlier. Furthermore, the sliding window may have an advantage when a fault is only seen a short amount of time. Assume that the fault is only seen in measurements 38 up to and including 42. Using the sliding window, there is at least one batch of 10 consecutive measurements that includes measurements 38 up to and including 42. When using the fully separated batch method, a maximum of 3 of the 5 faulty

measurements are taken into consideration in one of the batches. This could imply that the sliding window is better able to detect these kind of faults. The preceding considerations do not take into account the false alarm rate. Take the previous example. Assume that the confidence level is taken to be  $\alpha$ . The sliding window considers the batches of the fully separated batch method. Besides these batches, it considers more batches. This implies that on top of the false alarms related to the batches of the fully separated batch method, the sliding window can produce false alarms due to the other batches it uses. Hence, under the same chosen confidence level  $\alpha$ , the number of false alarms are on average larger when the sliding window is used than when the fully separated batch method is used. To overcome this, the confidence level used when utilizing the sliding window, should be taken higher than the confidence level used when using fully separated batches. Combining this with the observations in Section 3.2.2, the power of batches considered in both the sliding window approach as well as the fully separated batches approach, is lower in the case when the sliding window is utilized. As a consequence, the power of a hypothesis test using a specific batch is negatively influenced when using a sliding window instead of the fully separated batches approach. Furthermore, it is harder to determine the false alarm rate of the sliding window approach. For the fully separated batch method, this is an easy task. This is one disadvantage of the sliding window approach. These are considerations one can take into account when choosing to use the batch method or the sliding window method.

## E Extra Figures



(A)  $(\mu_1, \sigma_1^2) = (1, 0.5)$  and  $(\mu_2, \sigma_2^2) = (1.5, 0.5)$       (B)  $(\mu_1, \sigma_1^2) = (1, 5)$  and  $(\mu_2, \sigma_2^2) = (1.5, 5)$

FIGURE 13: The power of the test statistic  $Z$  as a function of the number of measurements per sample for different probabilities of a type I error  $\alpha$ . Two scenarios are treated

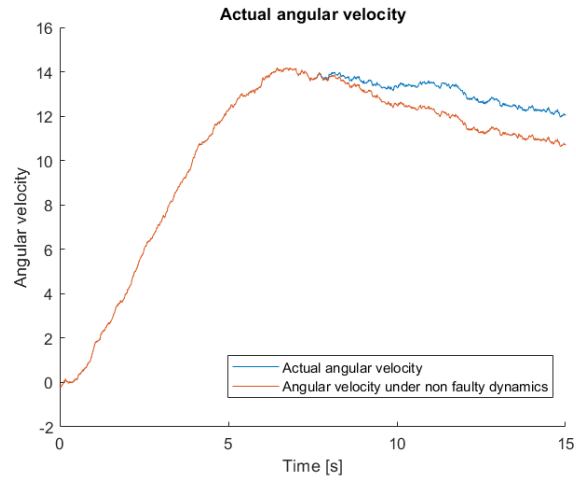


FIGURE 14: Actual angular velocity of a simulation when the resistance changes from  $R$  to  $100R$ . The assumptions as used to generate table 2 were used.

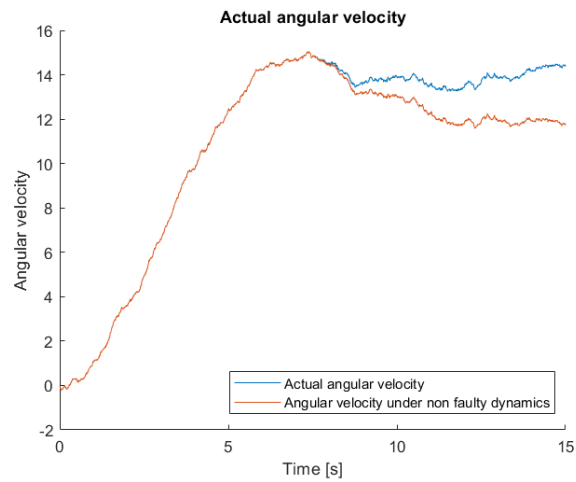


FIGURE 15: Actual angular velocity of a simulation when the inductance changes from  $L$  to  $100L$ . The assumptions as used to generate table 2 were used.

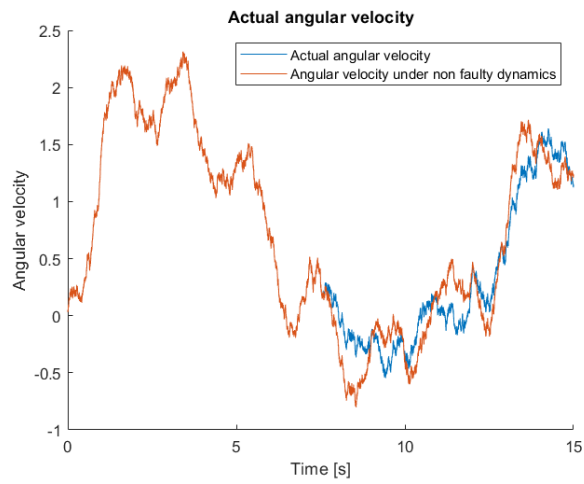


FIGURE 16: Actual angular velocity of a simulation of the 'Actuator fault: a loss of effectiveness' fault of table 2. The assumptions as used to generate table 2 were used.

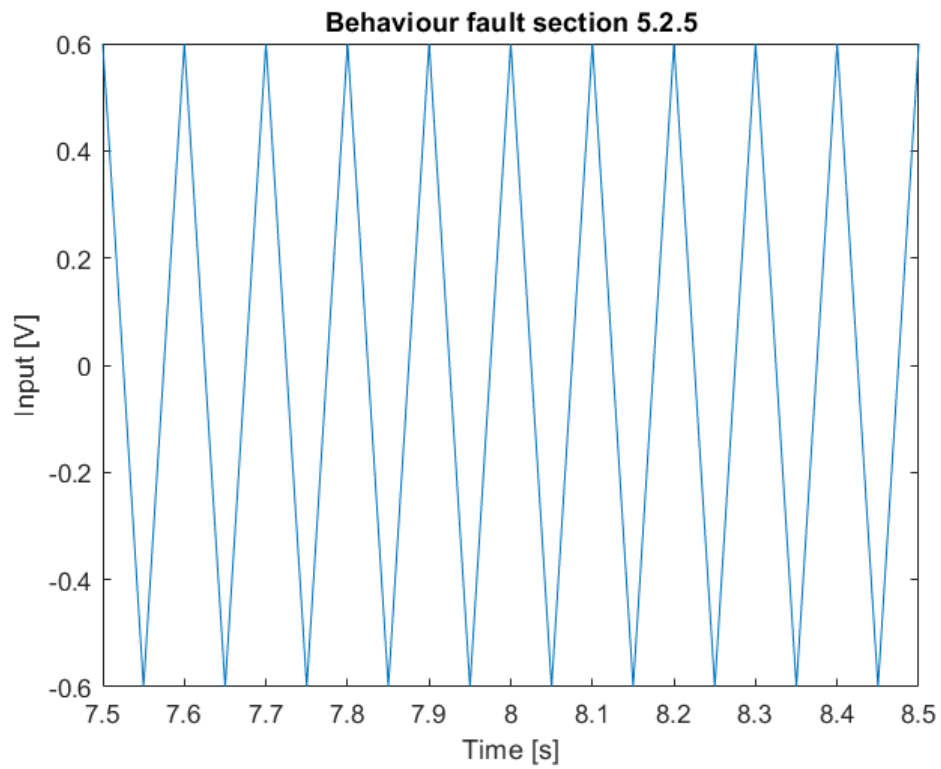
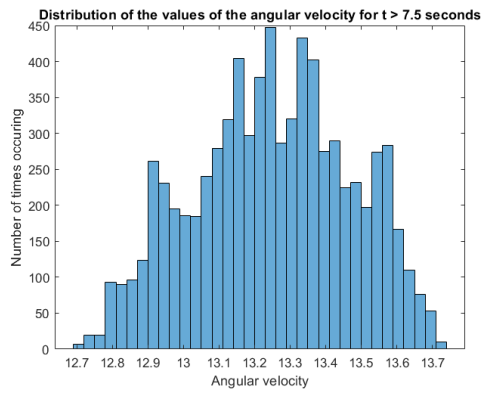
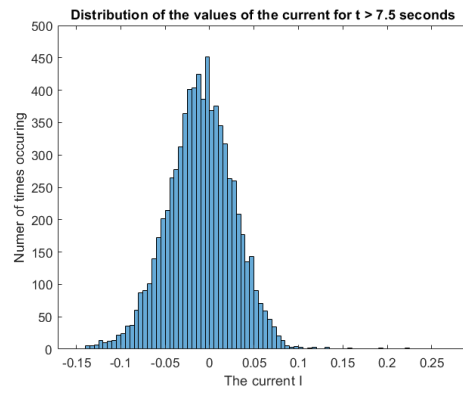


FIGURE 17: 10 periods of the extra fault input used for the simulations in Section 5.2.4.



(A) The distribution of the values of the angular velocity  $\omega$  for  $t > 7.5$  seconds



(B) The distribution of the values of the current  $I$  for  $t > 7.5$  seconds

FIGURE 18: Distributions of the values of the angular velocity and the current for  $t > 7.5$  seconds when the resistance changes from  $R$  to  $100R$  at  $t = 7.5$  seconds.

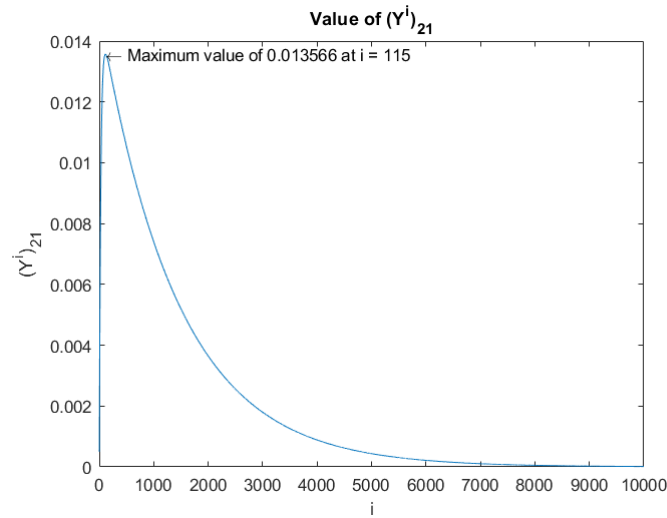
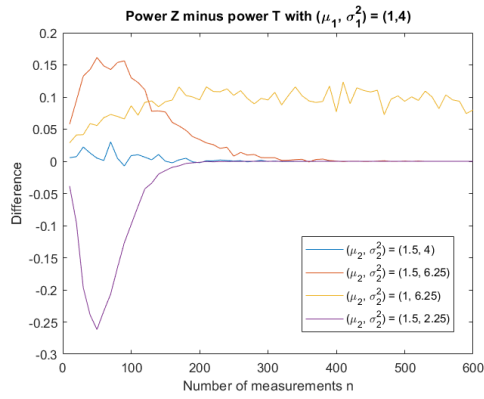
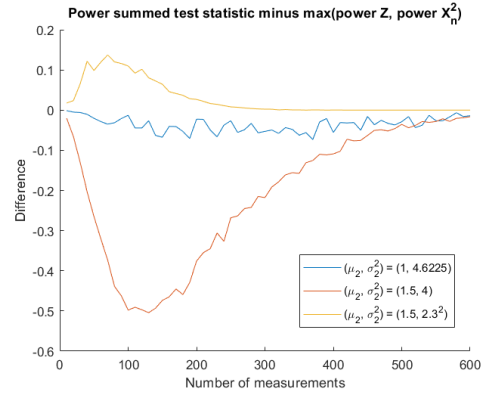


FIGURE 19: The values of  $(Y^i)_{21}$  for different values of  $i$  for the matrix  $Y$  given in Equation (21)

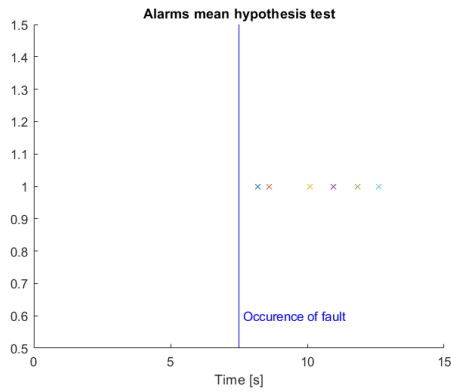


(A) Power  $Z$  minus the power of  $T$  for different fault scenarios

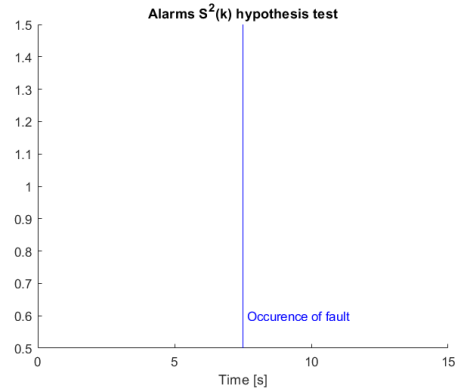


(B) Power of the summed test statistic minus the maximum of the power of  $Z$  and the power of  $X_n^2$  for different fault scenarios.

FIGURE 20: Comparing test statistics with  $(\mu_1, \sigma_1^2) = (1, 4)$ . Measurements are done every 0.1 seconds and an adaptive confidence level is chosen such that on average 1 false alarm occurs every 120 seconds

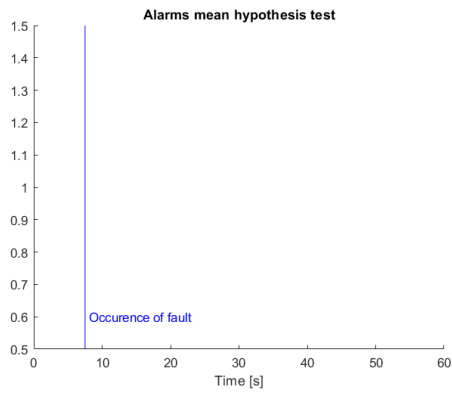


(A) Alarms of the  $\bar{X}(k)$  test statistic.

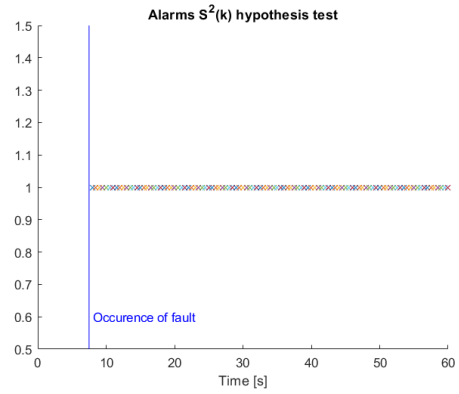


(B) Alarms of the  $S^2(k)$  test statistic.

FIGURE 21: The alarms given during a simulation of the 'More stochastic disturbance in the system' fault given in Table 4.

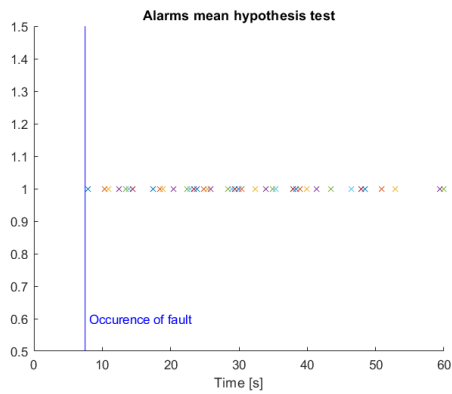


(A) Alarms of the  $\bar{X}(k)$  hypothesis test.

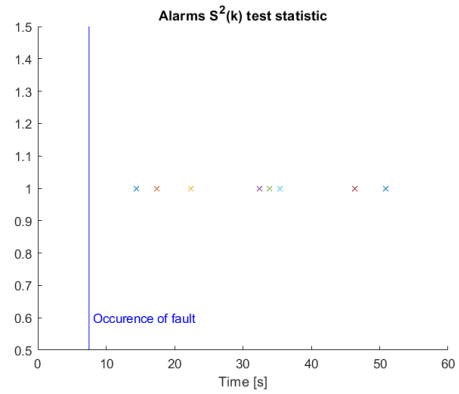


(B) Alarms of the  $S^2(k)$  hypothesis test.

FIGURE 22: Simulations with  $\Delta t = 0.001$ .



(A) Alarms of the  $\bar{X}(k)$  hypothesis test.



(B) Alarms of the  $S^2(k)$  hypothesis test.

FIGURE 23: Simulations with  $\Delta t = 0.1$ .